POLYVINYL ALCOHOL AS A STERIC STABILIZER

POLYVINYL ALCOHOL AS A STERIC STABILIZER

By

DILVA PADOVAN, B.Sc.

A Thesis

Submitted to the School of Graduate Studies

in Partial Fulfilment of the Requirements

for the Degree

Master of Engineering

McMaster University

MASTER OF ENGINEERING (1985) McMASTER UNIVERSITY

(Chemical Engineering) Hamilton, Ontario

TITLE: Polyvinyl Alcohol as a Steric Stabilizer

AUTHOR: Dilva Padovan, B.Sc. (Laurentian University)

SUPERVISOR: Professor D.R. Woods

NUMBER OF PAGES: xiii, 87

ABSTRACT

An experimental study of the steric stabilizing ability of a water soluble polyvinyl alcohol (PVA) polymer is presented.

The free film thickness of a lamella formed between a drop of n-butylchloride and bulk n-butylchloride stabilized by PVA was measured by the Hodgson and Woods technique in order to evaluate the stabilizing ability of the polymer. A maximum in the stability was observed as the concentration of the polymer was increased. This maximum trend can be explained by the HVO theory.

ACKNOWLEDGEMENTS

I wish to acknowledge and extend my gratitude to all those people who enabled me to complete this work.

I thank all the technicians in the Chemical Engineering Department at McMaster University for their helpful and unlimited assistance.

I wish to thank my supervisor, Dr. D.R. Woods, for all his patience and encouragement, without whose help this work was not possible.

I would like to acknowledge the funding I received from Imperial Oil Limited, who also provided me with the PVA polymer used throughout this study.

Finally, I wish to express my special thanks to my parents and husband for their limitless support.

TABLE OF CONTENTS

TABLE OF CONTENTS (continued)

TABLE OF CONTENTS (continued)

LIST OF FIGURES

LIST OF FIGURES (continued)

LIST OF TABLES

NOMENCLATURE

Q	partition function
F'	Helmholtz free energy
k	Boltzmann's constant
T	absolute temperature
i	number of segments
ι	average number of segments per chain
ℓ	length of a segment
$<\overline{r^2}>$	mean square end-to-end distance
χ	Flory-Huggins polymer-solvent interaction parameter
ν	number of adsorbed loops (or tails) per unit area
A	Hamaker constant
α	expansion parameter
V_s	volume of polymer segment
V_1	volume of solvent molecule
d	distance between two interfaces
h^2	surface area of a flat particle
ω	grams of polymer adsorbed per unit area
N	Avagadro's number
$\overline{M}$	average molecular weight of a polymer
v	excluded volume
j	layer number
z	coordination number of lattice
p_i	free segment probability in layer i with respect to the bulk solution

NOMENCLATURE (continued)

h_1	equivalent solution thickness of a film
h_f	polymer film thickness
s and s"	measure of distances along the chain contour
r and r"	positions in space
r	Fresnel coefficient
n_0	refractive index of air
n_f	refractive index of film
λ	wavelength of light
α''	angle of refraction
c	concentration
η_{sp}	specific viscosity
$[\eta]$	intrinsic viscosity
γ	interfacial tension
ρ	density
$\bar{\omega}$	angular velocity
y_o	semi major axis of the spinning drop
x_o	major axis of drop rotation
r	actual drop radius
α	dimensionless parameter
$\bar{M}_v$	viscosity average molecular weight
W	weight
w	width
t	thickness
B	buoyancy force

NOMENCLATURE (continued)

m	mass
a	acceleration due to gravity
f	force
$\bar{P}$	degree of polymerization
V	drop volume
T_s	Time elapsed from initial surface formation to drop release to bulk interface.
T_R	Time elapsed from time of drop release to coalescence.
T_E	Time elapsed from surface cleaning to drop release to bulk interface.
M	molecular weight of loop or tail.

CHAPTER 1

LITERATURE REVIEW, SCOPE AND OBJECTIVES

In suspensions and emulsions and in general dispersions of fine particles or drops in a liquid there are frequent encounters between particles due to Brownian movement, gravity, and convection. When the strong repulsive forces between the particles can counteract the attractive forces, and the particles remain free, then a dispersion is considered stable.

The attractive van der Waals interactions are of a relatively long-range character, of the order of 10 nm. Van der Waals attraction has been attributed to the interaction of dipoles, the polarizing action of a dipole in one molecule on another (induced dipole), and a quantum mechanical effect leading to an attraction between nonpolar molecules.

The repulsion can occur from an interaction between the electrical double layer, which gives rise to electrical stabilization, and from an interaction between the adsorbed layer of non-ionic materials (including adsorbed molecules of the dispersion medium), which gives rise to steric stabilization.

The objective of this thesis was to study the steric stabilization of n-butylchloride drops in water with polyvinyl alcohol (PVA) as stabilizer by varying the concentration of PVA, the drop volume, and the interface age independently.

1.1 Steric Stabilization

When a polymer adsorbs at an interface the segments which bind to the interface experience short range attractive forces. This lowers the free energy of the system. At the same time the polymer molecule loses entropy which tends to increase the free energy. As a result of these opposing forces only a fraction of the segments are bound to the interface (4).

These bound segments are referred to as trains. The other segments, which protrude into the solvent as loops and tails, experience intra- and intermolecular interactions between segments of adsorbed macromolecules. These interactions are to a large extent determined by solvent quality.

Polymers which provide the best stability seem to be block or graft copolymers which consist of both anchor groups and stabilizing moieties. The stabilizing moieties are soluble in the dispersion medium while the anchor groups are nominally insoluble. The mechanism of attachment of the anchor groups to the interface can have various origins such as van der Waals force of attraction, chemical, hydrogen, and hydrophobic bonding (35).

Schick and Harvey (39) studied the relationship between hydrodynamic dimensions of polystyrene in solution and its adsorption on Graphon. The amount of polymer adsorption was inversely proportional to the polymers cross sectional area in solution. The greater the difference in the solubility between the polymer and the solvent, the smaller the size of the polymer coil in solution and therefore the greater the adsorption (35, p. 16-19). A more solvated polymer has a larger radius of gyration.

Polymer adsorption is time dependent due possibly to diffusion, reconformation, and displacement. When a polymer reaches an interface it adsorbs via train segments. These adsorbed segments may exchange with non-adsorbed segments until the most advantageous conformation is obtained. The principal factors determining the conformation of the polymer at the interface are the flexibility of the polymer chain, the mutual interaction of the polymer segments and the interaction between the polymer and both the solvent and the interface. Vander Linden and Van Leemput (43) have shown that high molecular weight polymers adsorb preferentially over lower ones on a non-porous interface. Thus in polydispersed samples displacement of short molecules by longer ones may take place as time passes.

The direct determination of adsorbed polymer per unit area at liquid/liquid interfaces is not often very feasible, since as a rule the interface area is thin. Gibbs developed a thermodynamic equation relating the surface excess concentration of small molecules to the bulk molecular concentration and the reduction in interfacial or surface tension (see Appendix V).

Application of this equation to polymer systems is questionable because polymer adsorption is irreversible and one would not expect a theory based on equilibrium to apply. Lankveld (21, p. 10), however, applies the theory on the assumption that a local equilibrium occurs with reversibility for the adsorption of individual segments. This means that the calculated values may be interpreted in terms of the statistical chain element or segment (Appendix V).

1.2 Theories of Steric Stabilization

The first theoretical papers on steric stabilization were written in the 1950's by Mackor (26) and Fischer (12). Mackor calculated the loss of configurational freedom for a stiff chain adsorbed at one end on a flat particle with the approach of a second particle. This loss in entropy led to an increase in free energy and thus to repulsion.

Fischer (12) stressed the importance of an enthalpy contribution. He identified the cause of repulsion between particles covered by a polymeric layer to be the excess osmotic pressure in the region where these layers overlap.

Meier (27) was the first to recognize clearly the existence of both the volume restriction and the mixing, or osmotic, contribution to steric stabilization. Subsequently Hesselink, Vrij and Overbeek (17), HVO, refined these calculations via a statistical mechanical approach. Scheutjens and Fleer (37, 38) have presented a more sophisticated

statistical mechanical theory. These latter theories use a random flight model for the stabilizing moieties.

Dolan and Edwards (8,9) have also employed a random flight model. However, they treat the conformations as a random flight in the presence of a potential energy field that itself depends upon the solution of the random flight. All the contributions to the steric free energy are calculated simultaneously; they suggest that the artificial separation into mixing and elastic contribution, present in other theories, is avoided due to the self-consistent field approach.

It is still not possible to make accurate quantitative predictions of the potential energy in sterically stabilized systems. Two central problems remain unresolved; 1) the prediction of polymer conformations at an interface, 2) the thermodynamics of the interactions of two steric barriers.

The present theories used to explain steric stabilization are based on statistical thermodynamics. The difference between theories is mainly in the model underlying the partition function and the mathematical approximations applied in obtaining results. Once the partition function, Q, is formulated thermodynamic quantities can be derived. For example, the Helmholtz free energy F':

$$F' = kT \ln Q \qquad [1.1]$$

where k is the Boltzmann's constant and T the absolute temperature. The partition function has the form; $Q_j = \Omega_j \exp - E_j/kT$.

Theories which describe adsorbed macromolecules often make use of the Flory and Huggins polymer solution theory (11). In this theory the conformation of a chain molecule is calculated by placing the segments of the chain one by one in adjacent lattice sites. The sequence of steps constitutes a three dimensional random walk. The probability of each step is proportional to the probability of finding a vacant lattice site. When the local segment

concentration is assumed to be equal to the average solution concentration and all the steps are therefore assigned equal weighting, the walk is referred to as a 'purely random walk' and the theory is referred to as a 'mean field' theory. This theory is valid for relatively high concentrations where the polymer coils overlap extensively.

At low concentrations where the assumption of a homogeneous segment density does not apply, the conformational probability can be found from a 'self-avoiding walk'. A step is only allowed if the site is not occupied by a segment of the same chain.

When applying these ideas to adsorbed polymers, researchers assume that the segment density is constant parallel to the surface but varying perpendicular to the surface. Often a step perpendicular to the surface is weighted according to the local average segment density. This is called a 'step-weighted random walk'. Thus the conformational probability of an adsorbed chain can be described using the Flory and Huggins theory for polymer solutions.

In all the theories the polymer chain is represented by a sequence of i segments, all the same size and chemical properties and connected to each other by a flexible bond. The flexibility of this bond may or may not be subject to some constraint depending on the model. The definition of a segment varies with the model. However, the model chain must represent the statistical properties of the real chain. For example

$$\langle \overline{r^2} \rangle = i\ell^2 \qquad [1.2]$$

where $\langle \overline{r^2} \rangle$ is the mean square end-to-end distance of an isolated chain consisting of i segments of length ℓ.

The adsorbing surface is assumed to be divided into a number of identical adsorption sites, each of which can bind one segment.

Frequently spherical particles are modeled as flat plates for simplicity. This assumption is valid if the root mean square end-to-end distance of the adsorbing polymer is much less than the radius of the particle.

Polymer-solvent interactions are often accounted for by the Flory-Huggins interaction parameter χ. Where two χ equals the free energy in kT units associated with the exchange of one solvent molecule, in pure solvent, with an equal volume of polymer in pure polymer.

1.2.1 Model of Hesselink, Vrij, and Overbeek (HVO)

The HVO theory is based on Meier's theory (27). When two interfaces both covered by adsorbed polymer approach each other the resulting rise in interaction free energy, ΔF, is due to the sum of two effects; 1) a volume restriction repulsion, ΔF_{VR}, due to the decrease of configurational entropy of the adsorbed loops and tails on the approach of the second interface plus 2) an osmotic or mixing effect, ΔF_M, due to the mixing of the adsorbed polymeric clouds when the two particles approach, this effect can be attractive or repulsive depending on the solvent quality.

In general then the total change in free energy

$$\Delta F = \Delta F_{VR} + \Delta F_M + \Delta F_A \qquad [1.3]$$

where ΔF_A is the free energy of attraction due to van der Waals-London forces.

More specifically the equation derived by HVO (17) for the change in free energy per unit area when two flat particles approach each other is given by

$$\Delta F = 2\nu kT\, V(\tau,d) + 2(2\pi/9)^{3/2}\, \nu^2\, kT\, (\alpha^2-1)\, \langle r^2\rangle\, M(\tau,d) - A/12\pi d^2 \qquad [1.4]$$

where ν is the number of adsorbed loops or tails per unit area of surface, A is the Hamaker attraction constant, τ is the average number of segments per loop or tail and is related to the root mean end-to-end distance via $\tau\ell^2 = \langle r^2\rangle_o \alpha^2$, ℓ is the length of a segment, and α, the expansion parameter is related to the solvent quality. As the solvent quality increases so then does α. It is related to the Flory-Huggins interaction parameter χ by the following expression

$$\alpha^5 - \alpha^3 = \frac{27\, i^2 V_s^2 (1/2 - \chi)}{2\pi^{3/2} V_1 (i\ell^2)_o^{3/2}} \qquad [1.5]$$

where V_s and V_1 are the volumes of the polymer segment and solvent molecule respectively. Equation 1.5 assumes that an adsorbed polymer chain behaves the same as a free coil in solution.

$V(\tau,d)$ and $M(\tau,d)$ are exponential functions giving the rise in free energy per average loop (or tail) in units of kT. The adsorbed macromolecules are described by a self-avoiding random walk on a six-choice cubic lattice. No 'bridging' is allowed, i.e. no polymer is adsorbed on more than one particle. The form of the function changes with the mode of attachment of the macromolecule. They are functions of the distance between the two interfaces, d, and the experimental root mean end-to-end distance $\langle\overline{r^2}\rangle = i\ell^2$.

Figures 1.1 and 1.2 show $V(\tau,d)$ and $M(\tau,d)$ as functions of $d/\sqrt{i\ell^2}$ for particles covered by macromolecules attached by equal tails, loops, copolymers and homopolymers.

A more detailed description of this model is found in reference (17).

Figure 1.3 illustrates the overall free energy of interaction curve described by equation 1.4 as a function of distance d between two flat particles. At large values of d,van der Waals attraction predominates; as d decreases, the osmotic repulsion begins to influence the interaction, and finally at closer distances the volume restriction begins its influence. The depth of the minimum ΔF_m in the free energy curve determines the stability of the colloidal state. When the area of interaction h^2 times ΔF_m is greater than the thermal energy kT the particles will have a tendency to adhere. When $h^2\Delta F_m < 5$ kT simple stirring may redisperse the particles, $h^2\Delta F_m > 5$ kT the particles will remain together.

For spherical particles the influence of particle size on the energy of interaction will be less than for flat particles, since for spheres the stability is inversely proportional with the radius whereas for flat particles it is inversely proportional with h^2.

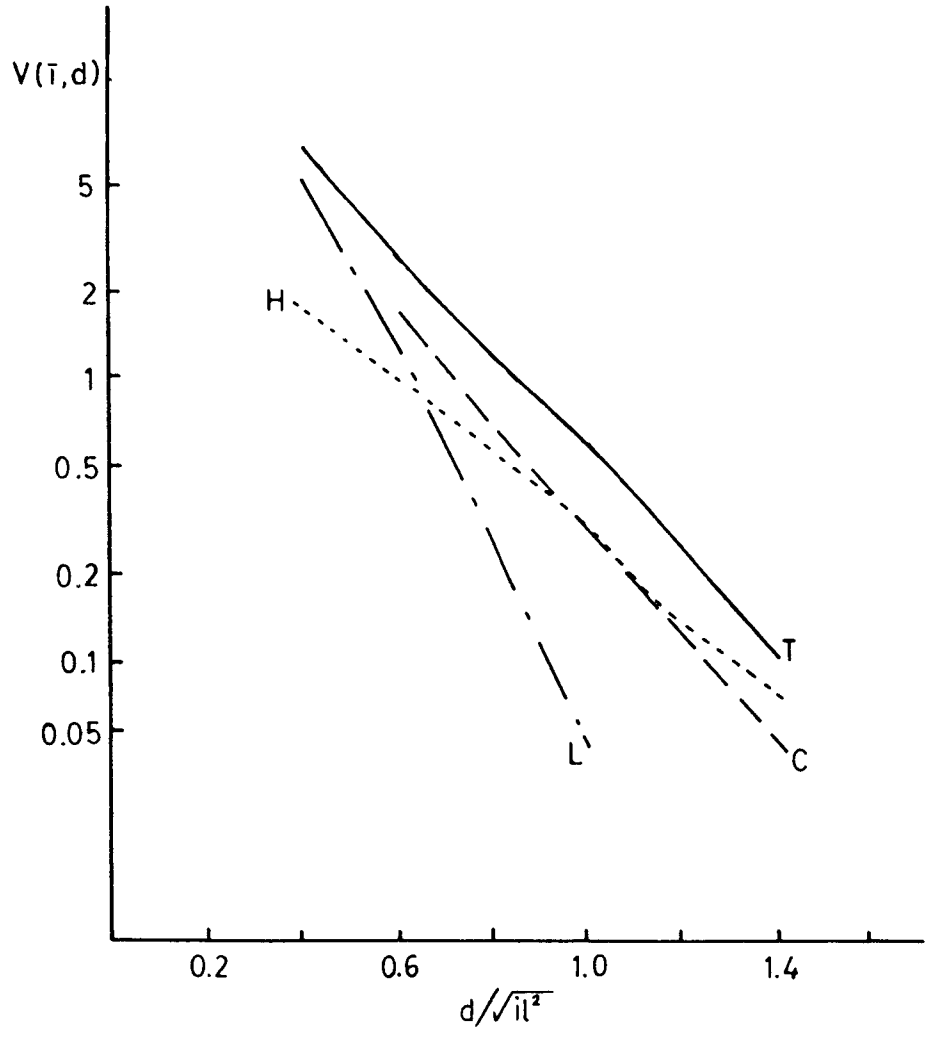

Figure 1.1 The rise in free energy per average chain length due to volume restriction imposed by a second interface at distance $d/\sqrt{il^2}$ (17).

H ------ homopolymer T ———— equal tails

C — — — copolymer L —— · —— equal loops

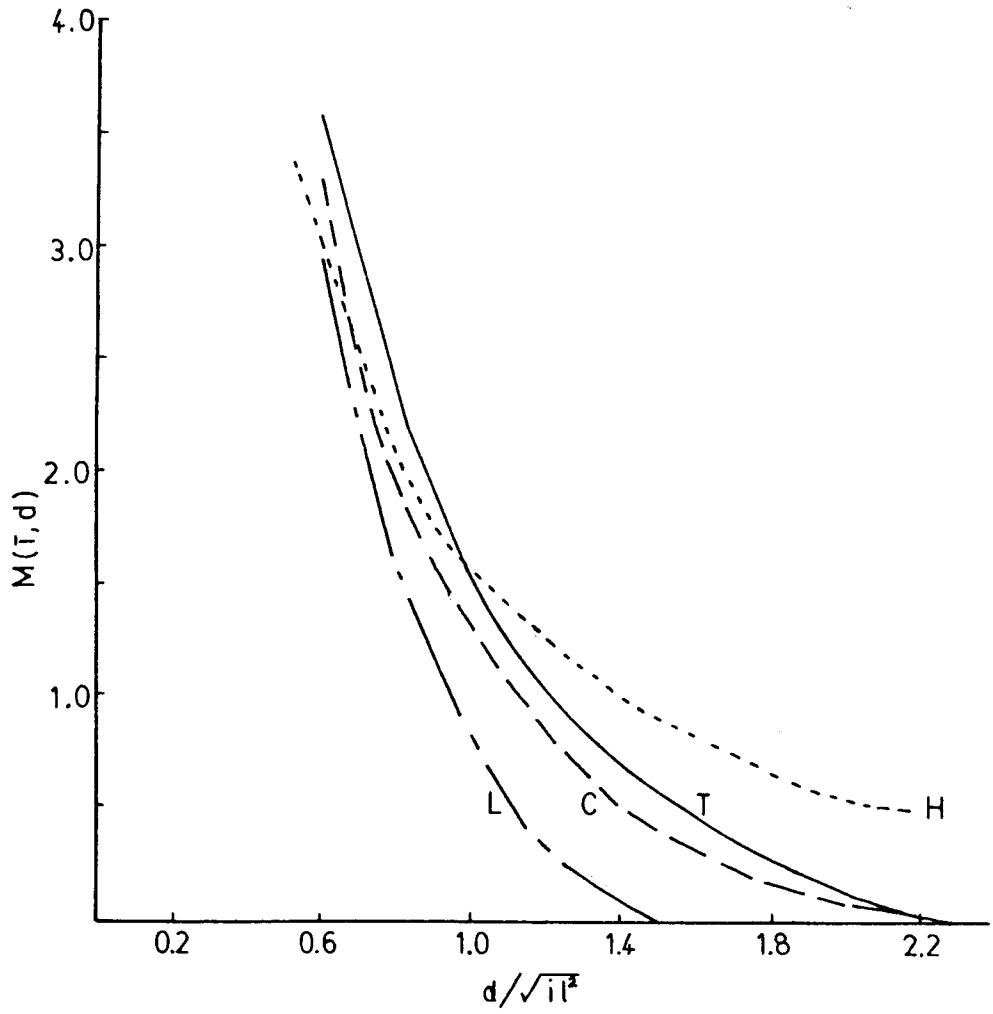

Figure 1.2 The dimensionless osmotic repulsion function $M(\tilde{\tau},d)$ for several modes of attachment of the polymer (17).

H ------- homopolymer

C — — — copolymer

T ———— equal tails

L ——.—— equal loops

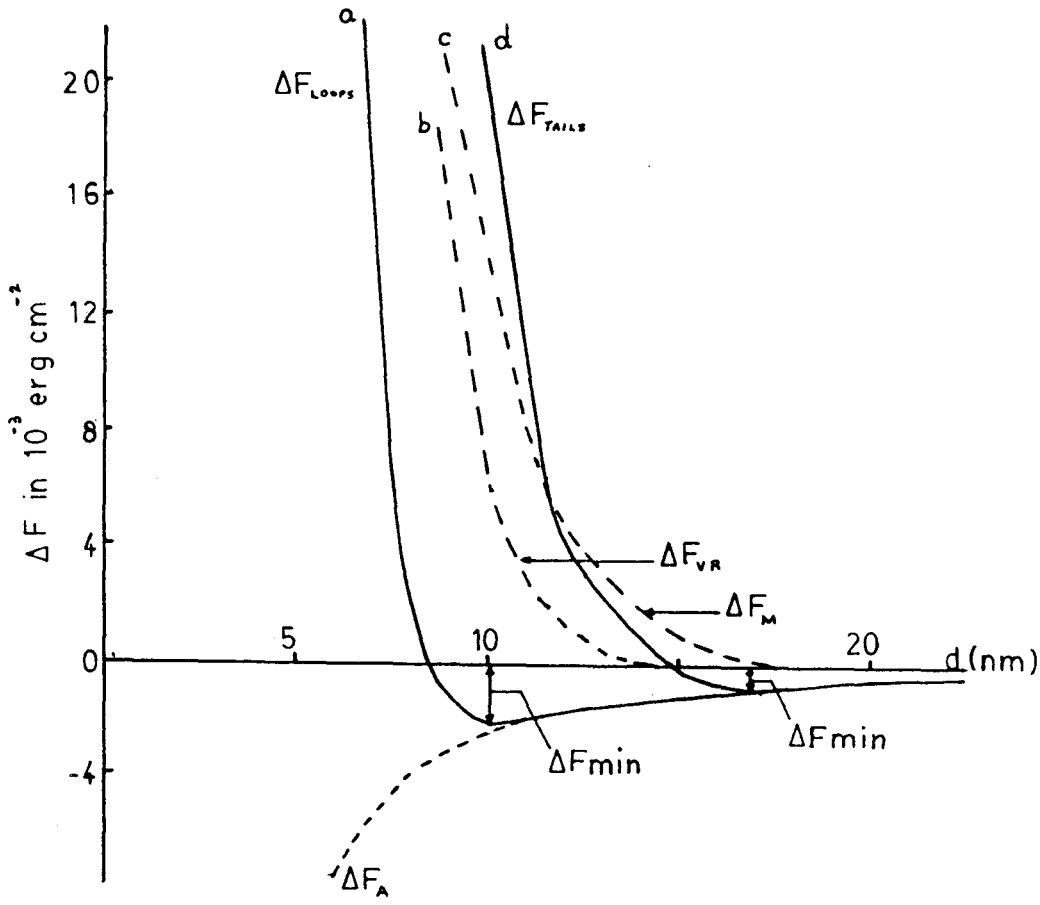

Figure 1.3 The free energy of interaction vs. the distance between particles (17).

a) overall free energy for particles covered by equal loops

b) volume restriction effect and c) osmotic pressure effect for particles covered by equal tails

d) overall free energy for particles covered by equal tails. Sum of curves b) and c).

$A=10^{-13}$erg, $\alpha=1.2$, $\omega=2\times10^{-3}$gcm^{-2}, $\bar{M}=6000$, $\langle\bar{r}^2\rangle^{1/2}=5.2$nm

Figure 1.4 shows the dependence of stability on the quality of the solvent (α) and on the amount of polymer adsorbed ($\omega = \sqrt{M/N}$). These curves represent $h^2\Delta F_m \simeq 5$ kT. To the right of these curves the systems are stable to the left unstable. As the solvent quality and/or the amount of polymer adsorbed decreases so then does the stability decrease. This phenomena has been confirmed experimentally (29,30). Curve (b) in Figure 1.4 curves back as the amount of polymer adsorbed is increased. For $\alpha < 1$ from equation 1.4, $\Delta F_m < 0$, and the osmotic effect thus causes an attraction. In this region of lower solvent quality at an intermediate value of polymer adsorption, the repulsion due to volume restriction prevails over both the van der Waals and osmotic attraction. Then, as the amount of polymer adsorbed is increased the system becomes unstable because the osmotic attraction increases faster than the volume restriction since ΔF_m is proportional to ω^2 and ΔF_{VR} is proportional to ω.

Generally, in a good solvent, this theory would predict that increasing the average molecular weight increases the stability. This is because highly extended layers cause repulsion when the particles are farther away from each other and the van der Waals attraction is still small.

Recently Hesselink (16) investigated the effect of a tail-size distribution on the free energy of interaction between two flat particles. He has shown, in Figure 1.5, that the interaction curve is less steep and of a wider range for the tail-size distribution than for equal tails.

In conclusion, the HVO model gives a satisfactory description of trends found by experimenters in sterically stabilized systems.

Napper et al. (10,28,29) have regarded osmotic repulsion as the mechanism of steric stabilization. They have argued that a proper formulation of the osmotic effect also takes into account the complete volume restriction repulsion.

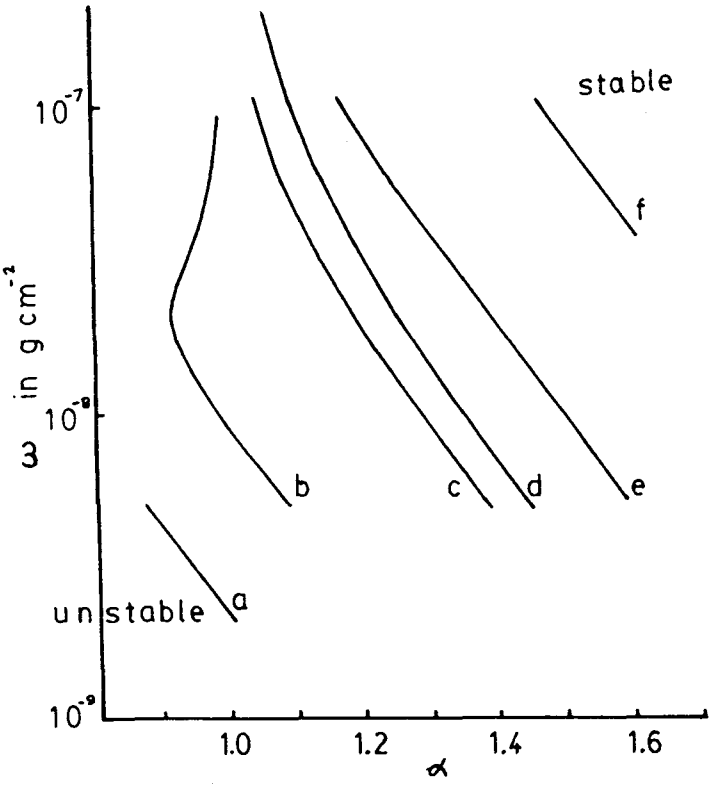

Figure 1.4 Dependence of stability on the quality of the solvent and on the amount of polymer adsorbed. To the right of the curve the system is stable, to the left it is unstable.(17)

a) $A=10^{-13}$erg, $\bar{M}=10^4$, h=0.1μm

b) $A=5\times10^{-13}$erg, $\bar{M}=6\times10^4$, h=0.1μm

c) $A=10^{-13}$erg, $\bar{M}=10^4$, h=0.2μm

d) $A=10^{-13}$erg, $\bar{M}=2000$, h=0.1μm
$A=5\times10^{-13}$erg, $\bar{M}=6\times10^4$, h=0.2μm

e) $A=5\times10^{-13}$erg, $\bar{M}=10^4$, h=0.1μm

f) $A=5\times10^{-13}$erg, $\bar{M}=10^4$, h=0.2μm

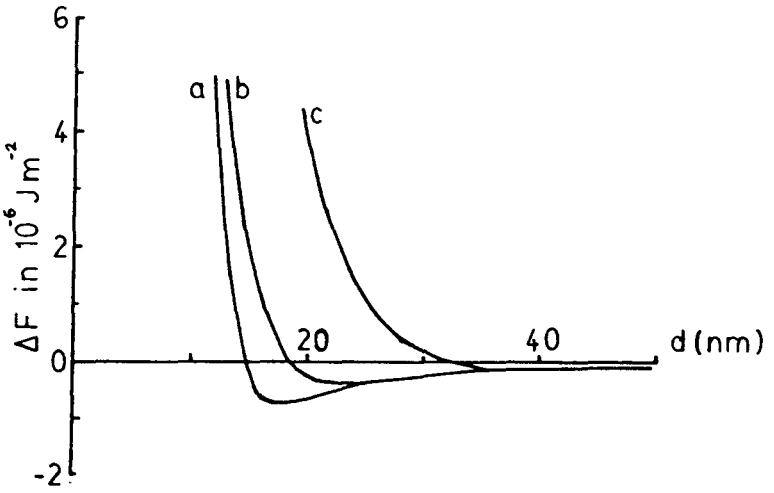

Figure 1.5 Effect of various modes of adsorption on the free energy of interaction between two parallel plates (16).

a) equal tails $\bar{M}$=6000. Tail

Tail size distibution $n_i \sim i^{-1/2} \exp(-i/2\langle i \rangle)$

b) $\bar{M}$=2000

c) $\bar{M}$=6000

Hesselink (16) has presented arguments which dispute Napper's claims. Napper's experimental observations are a specific case in the HVO theory. For example, Napper observed incipient instability for their latex systems stabilized with polymer at $\alpha \simeq 1.0$ irrespective of the length of the stabilizing tails. This behaviour can be explained by the HVO theory despite Nappers claims. At $\alpha < 1.0$ and with a surface coverage of $\omega = 2$ mg/m^2 no stability is predicted by HVO as was observed by Napper, since under these conditions the osmotic term governs the stability and it is attractive. At high and medium surface coverage, the osmotic term ΔF_M usually dominates over the volume restriction term ΔF_{VR} since, as explained earlier, ΔF_M is proportional to ω. Thus, Hesselink claims that the the majority of experimental results can be explained by the osmotic term.

1.2.2 Model of Dolan and Edwards

Doland and Edwards (8,9) extended the statistical calculations of the volume restriction effect to make allowance not only for restriction of configurational freedom caused by the second particle but also for the excluded volume due to polymer segments. The entropic and enthalpic interactions between solvated segments are thus taken into account without the artificial split of the free energy into two terms.

The configuration of a chain anchored at one end (tail) on one surface is treated as a random walk in the presence of a potential field which itself depends on the solution of the random walk. The method of solution is an iterative one. Starting with an approximate segment density distribution, they solve for the probability distribution from which a further approximation to the segment density is made and the process is repeated until a self-consistent solution is reached.

The self-consistent equation for the probability that a section of the chain which starts at (r',s') has its end at (r,s), G(rr',ss') is

$$(\partial/\partial s - 1/6\, \ell\nabla^2 + (v/\ell^2)\, p(r))\, G(rr',ss') = \delta(r-r')\, \delta(s-s') \qquad [1.6]$$

where $(1/\ell)\, p(r)$ is the segment number probability, ℓ is the length of a segment, and v is the excluded volume

$$v = (1/2 - \chi)\, V_s^2/V_1 \qquad [1.7]$$

where χ is the Flory-Huggins (12) interaction parameter for a given polymer and solvent and V_s is the volume of a segment and V_1 is the volume of a solvent molecule.

Once a satisfactory probability distribution is obtained, the number of configurations $\Omega(d)$ of the adsorbed polymer chains as a function of the separation distance, d, of the plane surface can be calculated. From this the free energy F(d) per polymer chain relative to when the surfaces are separated by a large distance D can be calculated.

$$F(d) = kT\, \ell n[\Omega(d)] - kT\, \ell n[\Omega(D)] \qquad [1.8]$$

They found their method was in close agreement with the HVO method at close separation distances $(d/(r^2)^{1/2} \leq 1.5)$ and for small values of the excluded volume.

The effect of the excluded volume is to flatten and broaden the segment density distribution compared to the distribution for random flight chains.

At close distances the repulsion force is due mainly to the reduction in the number of possible configurations of the polymer chains by the opposing surface. At farther distances the repulsion will be due mainly from the intermingling of the chains, assuming an appreciable excluded volume value, this will also reduce the number of available configurations.

Thus, according to the Dolan and Edwards model, HVO calculated the energy of repulsion to be too small at large separation distances since the excluded volume effect changes the polymer density distribution to a greater extent at larger separations and HVO assumed the distribution to be that for a random-flight polymer chain.

Dolan and Edwards conclude that the criterion for stability against looser association will be very greatly affected by the value of the excluded volume while the criterion for stability against close associations much less so. The stability of a colloid is thus most likely obtained with an appreciable value of the excluded volume.

1.2.3 Model of Scheutjens and Fleer

In this model (36,37,38) when the flat plates approach each other, part of the chains are adsorbed on both surfaces simultaneously (bridging). The fraction of bridges increases strongly with decreasing particle separation and at a distance comparable to the radius of the free coil, nearly all the chains form bridges. In very dilute solutions the attraction due to bridging results in adsorption flocculation. At higher concentrations, the segmental overlap and conformational entropy contribute most to the free energy and the system becomes sterically stabilized.

No assumptions are made about the segment distribution near the surface. The partition function is not written in terms of the concentrations of individual segments but in terms of the concentrations of chain conformations.

A lattice consisting of j = 1 to M layers parallel to the surface has lattice sites with z nearest neighbours (z = 6 for a cubic lattice). The central quantity in the theory is the free segment probability p_j. It expresses the preference of a free segment for a site in layer j over a site in the bulk solution. P_j contains an entropy factor, accounting for the fact that a fraction of sites in layer j is occupied by segments, an energy factor originating from the segment-solvent interaction, and an adsorption energy difference between segments and solvent molecules applicable only in the first layer j = 1.

$$p_j = \frac{\phi_j^0}{\phi_*^0} \exp\{2\chi(<\phi_i> - \phi_*) + \delta_{j,1}\chi_s\} \qquad [1.9]$$

where ϕ_j and ϕ_* are segment volume fractions in layer j, and in the bulk solution, the superscript 0 refers to the solvent volume fraction, $<\phi_j>$ is a weighted average of the segment density over the layers j–1, j and j + 1 (according to the coordination around a site in j), and $\delta_{j,1}$ is the Kronecker delta function. The quantity p_j is used as a weighting factor for each of the chain segments in layer j.

For a chain of i segments, a matrix formalism (7) for a random walk of i–1 steps is adapted, in which the weighting factor p_j is assigned to each segment. The probability of a chain conformation is proportional to the multiple product of i weighting factors. The conformation probability, from which the segment density is found, is also a function of that density profile therefore the solution can only be found by an iterative procedure by solving a set of m implicit simultaneous equations. The results depend on the type of lattice chosen, the evaluation of parameters such as χ_s, and, like most other models, on the definition of a segment. The volume of the polymer segment is equal to the volume of the solvent molecule; thus if the solvent is water the number of segments per chain will be very high and this may cause an overestimation of the number of possible conformations.

This model predicts that the segment concentration in the outer regions of the adsorbed layer is mainly due to tails, except in extremely dilute solutions. The tails determine to a large extent the average layer thickness and the interaction between polymer covered colloidal particles.

The free energy of interaction is a compromise between an attractive term due to bridging and a repulsive term caused by segmental overlap and conformational entropy losses. In dilute solutions (the ppm range) bridging dominates the free energy at particle separations of the order of the free coil radius which leads to flocculation. In concentrated solutions, the high segment concentrations in the overlap region gives rise to an overall entropic repulsion and therefore steric stabilization.

In a poor solvent the concentration of segments between two parallel plates is higher than in a good solvent, since segments attract each other.

1.3 Experimental Techniques used to Measure Liquid Film Thicknesses

Two experimental techniques will be discussed in this section. The first was used by Van Vliet (44) to measure the thickness of polymer stabilized free liquid films. The second technique was used by Hodgson and Woods (18) to observe liquid films thinning and was the technique employed in this thesis.

These techniques are used to study the formation of a thin liquid lamella between emulsion droplets and its eventual rupture.

The rate of thinning of the lamella depends on the viscosity of the continuous phase and on the rheological properties of the adsorbed polymer layer. For metastable systems the thickness of the lamella is mainly due to the intractions between the the two adsorbed polymer layers.

1.3.1 Technique of Van Vliet (44)

The liquid films were formed in a glass ring with an inside diameter of 3.7 mm and a height of 3 mm. The films were formed by bringing a droplet of polymer solution in the ring through a needle. The two surfaces could be brought together by suction, controlled by raising or lowering the container filled with polymer solution. The horizontal films had a diameter between 1.5 mm and 3.0 mm depending on the disjoining pressure (net force per unit area acting in the direction normal to the two parallel interfaces). The whole system was in

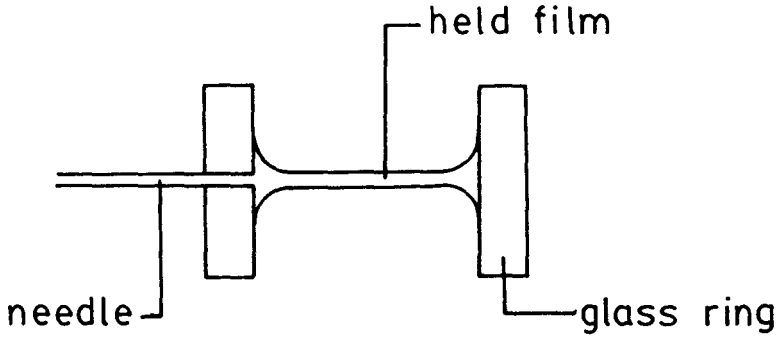

Figure 1.6 Glass ring with held film used by Van Vliet (44).

a temperature controlled box at 25.00°C. A diagram of the film is depicted in Figure 1.6. Thus, the films being studied were constrained by the bounding glass ring.

The thickness of the film was measured from the intensity of reflected light. The light source was a helium laser with wavelength 632.8 mm. Half the light was directed perpendicular onto the film and the other half was used as a reference beam.

The relationship between the intensity of the reflected beam I_r and the equivalent solution thickness of the film h_1 is given by

$$\frac{I_r}{I_s} = \frac{1 + 2r^2}{1 - 2r^2 + 4r^2 \sin^2\left(\frac{2\pi n_f h_1 \cos\alpha''}{\lambda}\right)} \sin^2\left(\frac{2\pi n_f h_1 \cos\alpha''}{\lambda}\right) \qquad [1.10]$$

where I_s is the reflected intensity of a silvery film, r is the Fresnel coefficient for non-polarized light and angle $< 30°$ given by $r = (n_f - n_o)/(n_f + n_o)$, n_o is the refractive index of air, n_f is the refractive index of the film, λ is the wavelength in vacuum of the light used, and α'' the angle of refraction. To obtain the thickness of the film, a correction is applied to h, which accounts for the differing optical properties of the surface layer and the ensuing multiple reflections because of the inhomogeneity of the film.

Measurements were made on solutions containing polyvinyl alcohol polymer and 1M glycerol. The drainage time of the film varied between 1 to 6 hours. Initially all the films drained with a dimple until approximately 1.5 to 2 times the equilibrium thickness. After this stage the thinning of the film slowed down.

The parameters investigated were: hydrostatic pressure, molecular weight of the polymer, the concentration of the polymer, and the reduction of the initial waiting time. With this information they were able to construct potential energy vs. film thickness curves for different PVA samples. Comparisons were then made with the HVO theory.

1.3.2 Technique of Hodgson and Woods (18)

With this technique lamella films were formed between an oil drop and a bulk oil interface both in contact with an aqueous phase. Figure 3.5 illustrates the lamella as viewed from the side. Thus, these films were free and unbound. The drop was formed on a capillary tip and released through the aqueous phase to the oil interface. The liquids were contained in a glass cell equipped with a cleaning probe. Details of the experimental technique similar to that used by Hodgson and Woods are given in section 2.3.

White light was used to measure the lamella film thickness. The light was reflected perpendicular to the interface from the top of the cell. As shown by Lawrence (22), for soap films, color interference patterns can be related to the lamella thickness as the film thins. Table 2.1 lists the observed colors produced by the reflected light for various lamella film thicknesses.

The technique developed by Hodgson and Woods has the distinct advantage of resembling a real system. It is also a simpler system. However, the lamella thickness can only be determined to within ± 20 nm, unless monochromatic light and thus a light intensity method was used.

1.4 Objectives of Research

There were two general objectives of this research:

1) To determine if the method of Hodgson and Woods (18) could be used to evaluate the stability of n-butyl chloride drops, covered with a water soluble non ionic PVA stabilizer, by varying the PVA concentration, the n-butyl chloride drop volume, and the interface age independently. How did the van Vliet method (44) compare with the Hodgson and Woods method?

2) To determine how much information could be obtained about the PVA/n- butyl chloride interface through interfacial tension measurements, measured with time and as a function of the PVA concentration. Could the Gibb's adsorption isotherm equation be used to evaluate the excess PVA at the interface?

CHAPTER 2

EXPERIMENTAL

2.1 Materials

The materials used in this study were chosen to simulate those pertinent for industrial polymerization of vinyl chloride with polyvinyl alcohol as stabilizer.

N-butyl chloride was chosen as the organic analog to vinyl chloride without the health hazard and experimental problems associated with vinyl chloride. The butyl chloride was a Baker Analyzed reagent with a density of 880 kg/m^3 at 25°C and with a refractive index of 1.4021 at 20°C (5) and Baker TM Grade (98% minimum assay). The latter was used more extensively except were indicated. The interfacial tension between n-butyl chloride and water was measured as 32 ± 13 mN/m at 25°C via the spinning drop method and 30.5 ± 3 mN/m via the Wilhelmy plate method.

Generally, PVA is prepared by polymerizing vinyl acetate to polyvinyl acetate (PVAc) and subsequently partially hydrolyzing the polymer (21)

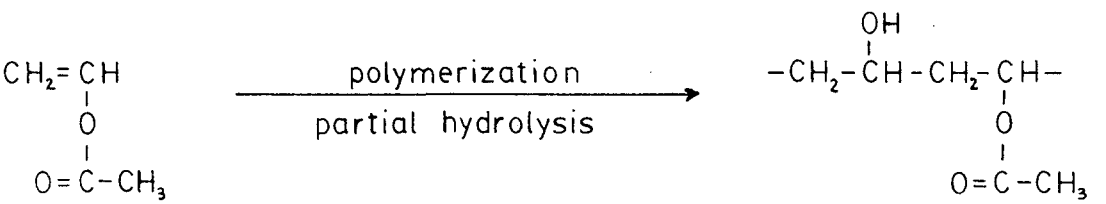

The polyvinyl alcohol (PVA) used in this study was obtained from Imperial Oil.

Aqueous solutions of PVA are stable, although fully hydrolyzed PVA in concentrated solutions can aggregate after time (41). A commercial product PVA-KZ-04 was used in this work. When preparing solutions of the PVA-KZ-04 it was found that to ensure complete dissolution, the solution should stand overnight. The solubility in water at 20°C was

about 0.8 g/dL. The solubility decreased with increasing temperature. PVA is insoluble in n-butyl chloride.

The viscosity average molecular weight for PVA-KZ-04 was 23,300 with the degree of polymerization equal to 400 and the degree of hydrolysis equal to 72.0 mol percent (28% acetate content) (34).

The PVA polymer is considered to be a nonionic polymer. Although the conductivity of the PVA-KZ-04 solutions increased slightly with concentration (for a 0.1 g/dL increase in concentration, the conductivity increased 16.3 micromho cm^{-1}) and attempts to determine the zeta-potential of butyl chloride drops covered with the PVA were unsuccessful, it was assumed that the increase in conductivity was due to a contaminant.

The intrinsic viscosity of PVA-KZ-04 was determined by plotting η_{sp}/c vs. c and extrapolating to zero concentration; the value was $[\eta] = 0.229$ dL/g (Appendix I). From this value the root-mean-square end-to-end distance of the polymer in water was estimated to be $(\overline{r^2})^{\frac{1}{2}}_{25°C} = 13.6$ nm (Appendix I), which is in agreement with Van Vliet's work (44).

The water used throughout this study was distilled and then passed through two carbon filters, a deionizing column and finally a millipore filter. The final conductivity of the water was less than one micromho and only trace amounts of organics were detected by liquid chromatography (33). The purified water was stored in a stoppered glass container.

2.2 Cleaning Procedure

To prevent surface contamination, all glassware and teflon which came into contact with either the n-butyl chloride or the water phase were thoroughly cleaned as follows:

1) washed in an ultrasonic bath with hot soapy water.

2) rinsed thoroughly with tap distilled water.

3) soaked in chromerge (chromic-sulfuric acid)for more than four hours.

4) rinsed and/or soaked with approximately 50% phosphoric acid/purified water.

5) rinsed throughly with purified water.

6) drained and stoppered all open ends with kimwipes.

The clean glassware was used within two weeks of cleaning. Gloves were worn whenever clean glassware was handled.

2.3 Film Thickness Measurements Between a Butyl Chloride Drop and a Surface Stabilized by PVA

The technique used to measure the free film thickness of the PVA stabilized films was first developed by Hodgson and Woods (18) and later expanded by Liem (23).

2.3.1 Apparatus

A schematic diagram of the apparatus used to determine film thicknesses is shown in Figure 2.1. The apparatus was made of glass with teflon stopcocks and was mounted on plywood which was in turn mounted on a cement block resting on rubber pads in order to prevent building vibrations from interfering with the measurements. The temperature of the room was 23.5 $\pm$ 1.5°C.

Once dismantled, the apparatus was easily cleaning according to the procedure listed in section 2.2, and then reassembled as described in Appendix II.1.

2.3.2 Procedure

Variables controlled during the experimentation were: 1) the bulk polymer concentration in the cell, 2) the n-butyl chloride drop size, 3) the interface age.

Figure 2.1 A schematic diagram of the apparatus used to determine film thickness.

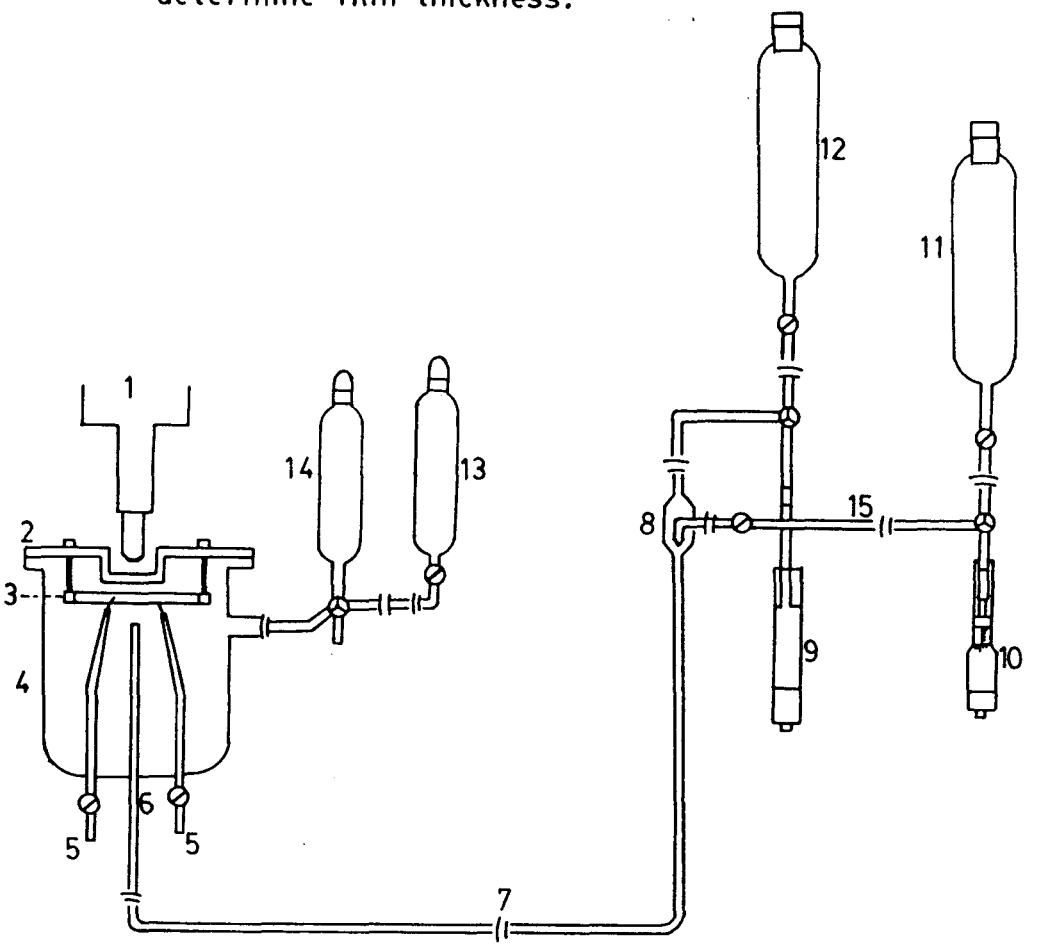

1 microscope with camera
2 cell cover with depression for microscope oil
3 teflon ring and screws
4 cell
5 cleaning probe with teflon tip insert
6 drop carrying tube
7 connecting tube
8 drop forming device
9 syringe
10 alga syringe
11 organic reservoir
12 aqueous reservoir
13 organic reserve
14 aqueous reserve
15 connecting tube

⊘ two-way stopcock
⊛ three-way stopcock
(ı ball & socket joint

Each PVA concentration was prepared by weighing the KZ-04 polymer into a volumetric flask. The flask was then partially filled with water, shaken repeatedly, and then allowed to stand overnight to ensure that the polymer had completely dissolved.

The drop formation procedure is listed in Appendix II.2. The interface age was measured with a stopwatch from the time of interface cleaning (see Appendix II.2, step 7) which was done before each drop was released to the interface. The drop volumes were varied between 0.6 μL and 3.6 μL.

Once the drop was released to the interface the thinning of the lamella film between the drop and the bulk interface was measured by observing the reflected white light. Interference color patterns were observed through the microscope and/or photographed on colored slide film, 160 Tungsten ASA, with a Pentax camera mounted on the microscope with an objective of magnification ten. The relationship between the interference color and film thickness is shown in Table 2.1 (3). This method of using color to determine thickness was first developed by Lawrence in 1929 (22). A detailed description of how a lamella thickness can be obtained from light interference colours is presented in Burrill's work (3).

2.4 Interfacial Tension by the Spinning Drop Method

When a drop of fluid, placed in a higher density liquid, is subject to rotation in a horizontal tube, it becomes elongated along the axis of rotation. This deformation shape can be related to the interfacial tension between the two fluids, since the centrifugal force is balanced by the interfacial tension.

Vonnegut (45) first suggested an approximate theory which related drop dimensions and speed of rotation to interfacial tension

Table 2.1 Interference colour and film thickness relationship, for films with a refractive index of 1.33.[1] (3)

Colour	Thickness[2]
First order	
black	0.2 - 0.4
grey	0.4 - 0.8
white	0.8 - 1.2
brown (straw)	1.2 - 1.4
brown (dark)	1.4 - 1.8
purple	1.8 - 2.2
Second order	
purple	2.2 - 2.3
blue (dark)	2.3 - 2.5
blue	2.5 - 2.7
green (bluish)	2.7 - 2.9
green	2.9 - 3.2
green (yellowish)	3.2 - 3.3
yellow	3.3 - 3.5
orange	3.5 - 3.7
red (crimson)	3.7 - 3.9
Third order	
purple (deep)	3.9 - 4.1
purple	4.1 - 4.3
blue (dark)	4.3 - 4.4
blue	4.4 - 4.6
green (bluish)	4.6 - 4.8
green (emerald)	4.8 - 5.1
green (yellowish)	5.1 - 5.5
red (carmine)	5.5 - 5.9
red (bluish)	5.9 - 6.2
Fourth order	
green (grass)	6.2 - 6.5
green	6.5 - 7.0
yellow (greenish)	7.0 - 7.5
red (carmine)	7.5 - 8.3
Fifth order	
green	8.3 - 9.2
pink	9.2 - 10.3
Sixth order	
green	10.3 - 11.2
pink	11.3 - 12.4
Seventh order	
green	12.4 - 13.5
pink	13.5 - 14 7

Note

1) to convert the table for films with a refractive index of n, multiply the thickness by (1.33/n)
2) in thousands of Angstroms

$$\gamma = \frac{\Delta\rho\ \bar{\omega}^2\ y_o^3}{4} \qquad [2.1]$$

where $\Delta\rho$ is the density difference between the two fluids, $\bar{\omega}$ is the angular velocity in rad, y_o is the semi major axis of the spinning drop, and γ the interfacial tension at temperature T.

This equation, however, is only applicable at very high speeds of rotation since it assumes a tubular drop shape. The theory has since been improved to include calculations at lower speeds as well.

Princen's et al. method (32) was used to calculate interfacial tension in this study. With this method, the drop volume was measured accurately in order to determine the radius of the drop, r. The cylindrical coordinate of the major axis of the rotating drop, x_o, and the angular velocity, $\bar{\omega}$, were measured on the spinning drop apparatus. Since x_o/r was always less than 2.209, equation [2.2] and Table 2.2 (32) were used to calculate the interfacial tension according to Princen et al.

$$\gamma = \frac{\Delta\rho\ \bar{\omega}^2\ a^3}{2\alpha} \qquad [2.2]$$

where a is the radius of curvature of the drop surface at the origin and is obtained from Table 2.2 and α is a dimensionless parameter obtained from Table 2.2. Both parameters depend on the value x_o/r.

2.4.1 Apparatus

A diagram of the spinning drop appaatus is shown in Figure 2.2. It is equipped with a microscope and vernier to measure the drop dimensions, a temperature controlled sample casing, and a fractional horsepower motor used to rotate the sample tube.

Table 2.2 Shape parameters of a rotating drop calculated by Princen, Zia, and Mason (32).

α	r/a	cr^3	x_o/r	y_o/r	x_o/y_o
0	1.000	0	1.000	1.000	1.000
0.05	1.017	0.0263	1.009	0.996	1.013
0.10	1.037	0.0557	1.018	0.990	1.028
0.15	1.058	0.0888	1.029	0.985	1.044
0.20	1.081	0.1265	1.042	0.980	1.063
0.225	1.095	0.1476	1.048	0.976	1.074
0.250	1.108	0.1703	1.056	0.973	1.085
0.275	1.124	0.1951	1.063	0.969	1.098
0.300	1.140	0.2222	1.072	0.965	1.111
0.325	1.158	0.2521	1.082	0.060	1.126
0.350	1.177	0.2854	1.092	0.955	1.143
0.375	1.198	0.3227	1.104	0.950	1.162
0.400	1.222	0.3653	1.117	0.944	1.184
0.425	1.250	0.4146	1.132	0.937	1.209
0.450	1.281	0.4727	1.150	0.928	1.238
0.475	1.318	0.5435	1.171	0.919	1.275
0.500	1.363	0.6330	1.198	0.907	1.321
0.525	1.421	0.7536	1.234	0.892	1.384
0.550	1.504	0.9354	1.287	0.869	1.481
0.555	1.526	0.9854	1.301	0.863	1.508
0.560	1.550	1.043	1.318	0.857	1.539
0.565	1.578	1.111	1.338	0.849	1.576
0.570	1.611	1.192	1.361	0.840	1.621
0.575	1.652	1.296	1.390	0.828	1.678
0.580	1.704	1.435	1.429	0.814	1.756
0.5825	1.737	1.528	1.455	0.804	1.809
0.5850	1.779	1.648	1.488	0.792	1.878
0.5875	1.836	1.817	1.534	0.776	1.977
0.5900	1.925	2.105	1.613	0.751	2.148
0.5910	1.986	2.314	1.669	0.734	2.275
0.5920	2.099	2.739	1.781	0.702	2.538
0.5922	2.150	2.944	1.834	0.688	2.667
0.5924	2.217	3.227	1.907	0.670	2.846
0.5925	2.289	3.555	1.990	0.651	3.059
0.59255	2.355	3.869	2.068	0.634	3.261
0.59257	2.412	4.161	2.140	0.620	3.452
0.59258	2.468	4.453	2.209	0.606	3.645

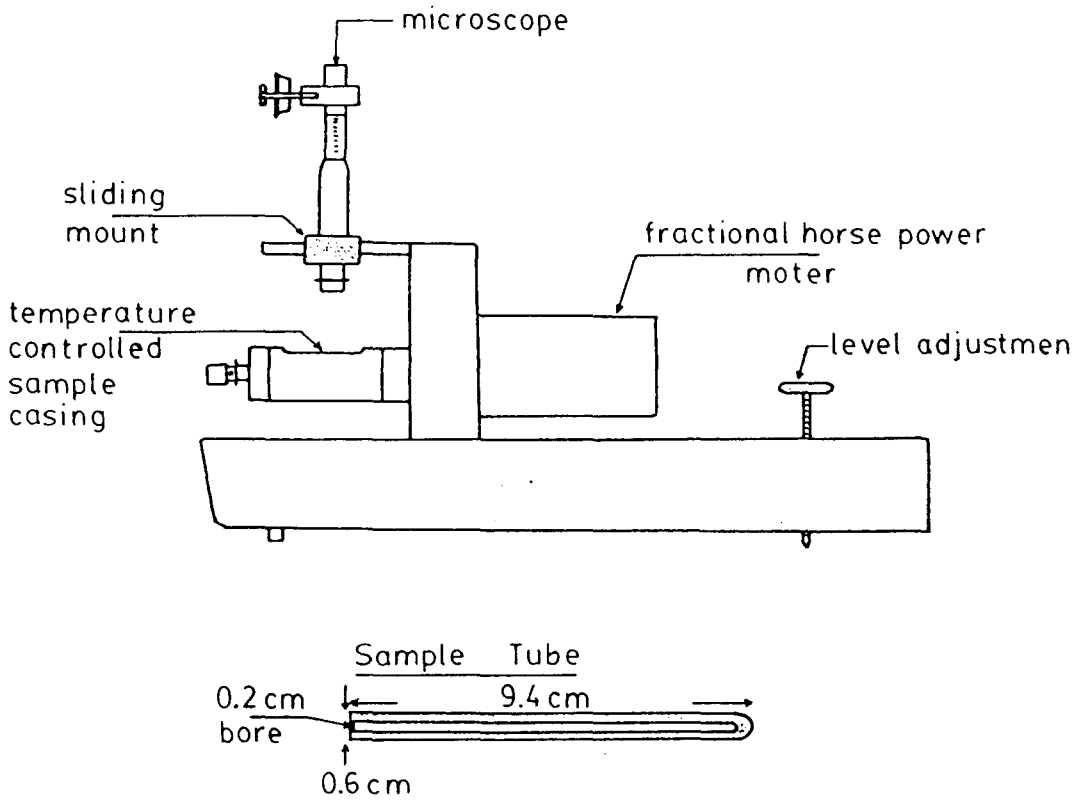

Figure 2.2 Spinning drop apparatus with sample tube

2.4.2 Procedure

The glass sample tubes were washed according to the standard procedure listed in section 2.2 before every run. A PVA solution, prepared form a 0.0150 g/dL stock by dilution, was injected into the glass tube, filling the tube completely. Then, a drop of butyl chloride, usually 1.5 μL in volume, was introduced into the PVA solution with a 10 ± 0.1 μL Hamilton syringe. No air bubbles were present. The tube was then placed into the temperature controlled casing of the spinning drop apparatus. The spinning drop dimensions along with the rotation speed (3800 rpm to 4300 rpm) were measured and the interfacial tension calculated according to equation 2.2.

The method lent itself very well to a time study, since the drop interface was not disturbed, except for deformation during the interfacial tension measurement.

The error theoretically inherent in this method is depicted in Figure 2.3. As x_o/r approaches 1.0, the error becomes exponentially large.

The interfacial tension between the PVA solutions and n-butyl chloride were also determined by the Wilhelmy plate method (Appendix III) and the Drop weight method (Appendix IV).

2.5 N-Butyl Chloride Emulsions Stabilized by PVA

Ten milliliters of PVA solution was placed in a 2.7 cm wide test tube and 10 milliliters of n-butyl chloride was then poured on top. The emulsions were prepared by mixing the solution with a propeller for approximately one minute. This procedure was performed for three concentrations of PVA; 0.006 g/dL, 0.03 g/dL and 0.06 g/dL.

Figure 2.3 Error in γ as a function of x_o/r given $\Delta\rho$ = 0.114 g/mL and $\bar{\omega}$ = 439 rad/s ± 10 rad/s

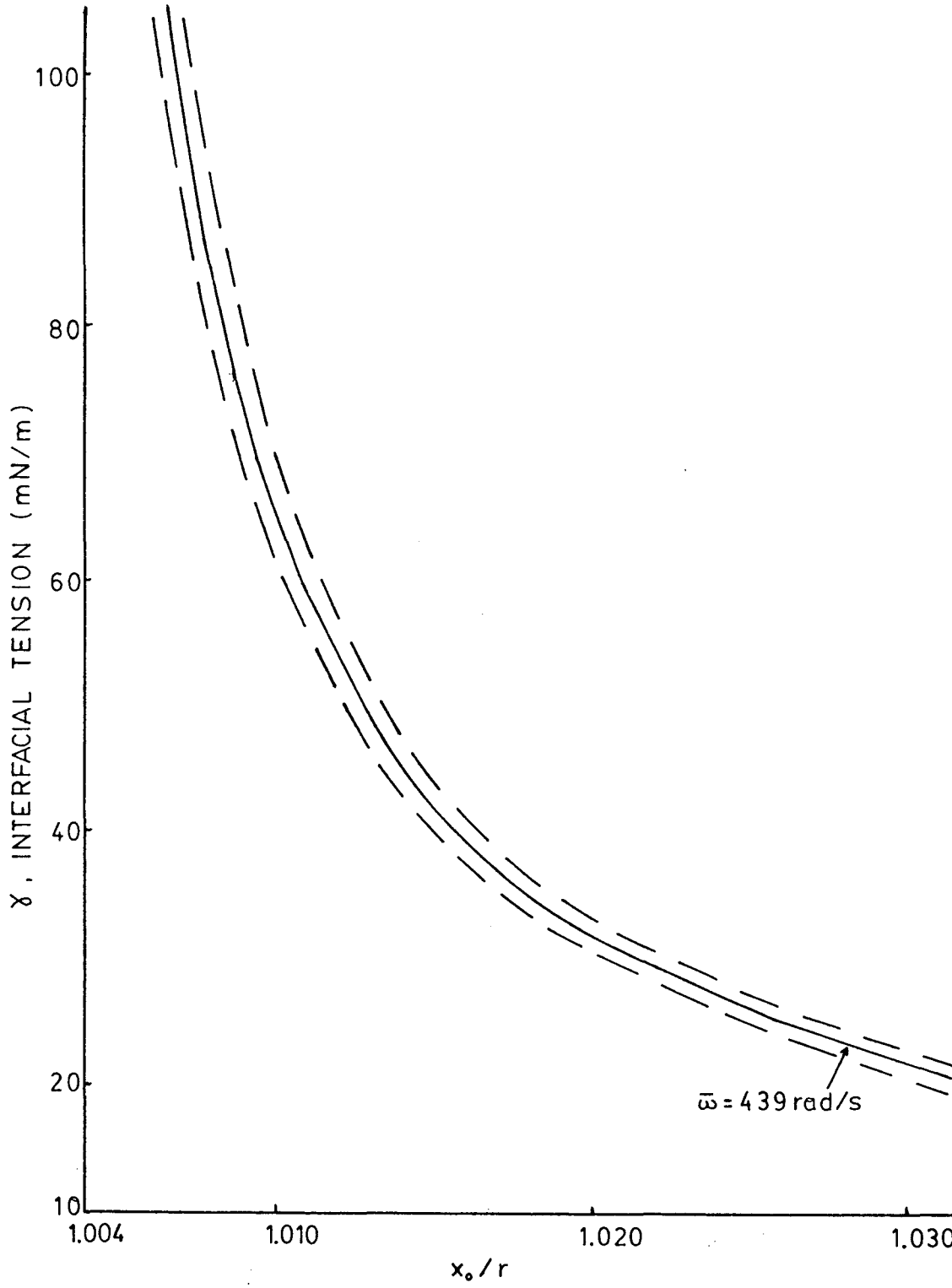

CHAPTER 3

RESULTS AND DISCUSSION

From the measurements of interfacial tension, film thinning and emulsion stability, information about the applicability of the methods used in this study and the relationship of the observed results to theory are explored.

3.1 Time-Dependency of Interfacial Tension

The interfacial tension of polymer solutions/oil systems have been found to depend on time (21). This time-dependency has been attributed to 1) the rate of supply of the polymer to the interface by diffusion, and 2) the rate of reconformation of the polymer in the interface once it is adsorbed.

The method used to measure the change in the interfacial tension affects the results. Lankveld (21) has demonstrated that when the interfacial tension is measured by methods which disturb the interface, not only is the size of the measured reduction influenced, but also the observed steady-state is reached much more quickly than with methods which do not disturb the interface.

Figure 3.1 compares three methods used in the current work to measure the interfacial tension of PVA solutions/n-butyl chloride as a function of concentration. The drop weight method, with drop formation time equal to approximately 2 minutes, was used to produce curve (a); the dynamic Wilhelmy plate method, with measurements taken half an hour after interface formation, produced curve (b); and the spinning drop method, with measurements taken 15 hours after interface formation, produced curve (c).

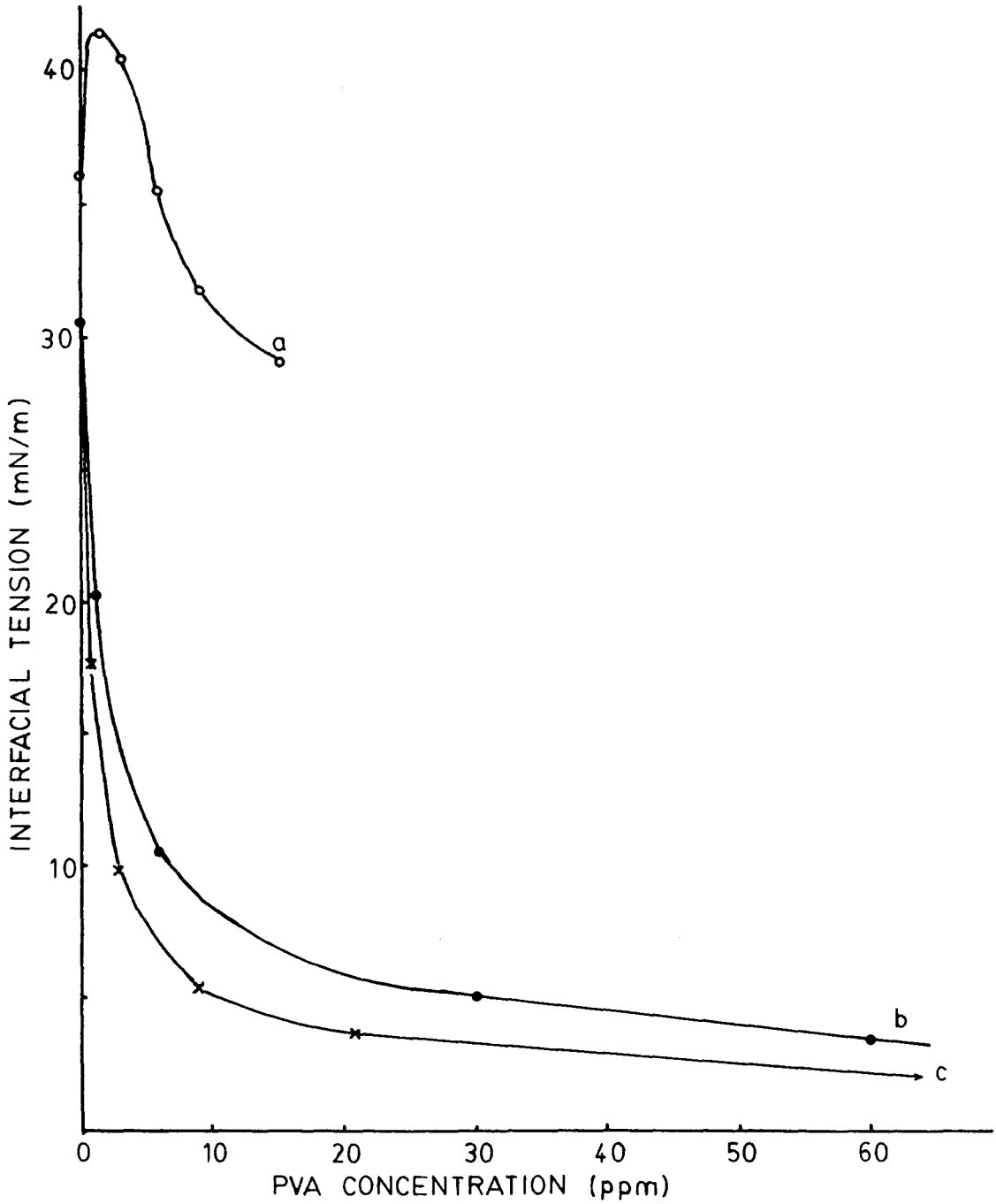

Figure 3.1 The interfacial tension between n-butyl chloride and PVA solutions vs. PVA concentration.

a) Drop weight method

b) Wilhelmy plate (½ hour after interface formation)

c) Spinning drop (15 hours after interface formation)

The drop weight method is inappropriate for studying polymer absorbing surfaces. As the drop forms on the capillary tip, a new surface is constantly being created where polymer may adsorb. Steady-state may never be reached before the drop falls.

Since the spinning drop method required the longest time for the interfacial tension to reach steady-state and exhibited the largest drop in the interfacial tension, this method was chosen to provide the most reliable values of interfacial tension.

The interfacial tension measured by the spinning drop method at different times after interface formation is given in Figure 3.2 for various concentrations of PVA.

The time-dependency of the interfacial tension was attributable to either diffusion or to reconformation at the interface from the equation:

$$\gamma_t = \gamma_o - \underbrace{2\nu c_p k T \sqrt{D/\pi}}_{\beta_1} \sqrt{t} \qquad [3.1]$$

where γ_t is the interfacial tension at time t, γ_o is the interfacial tension at time $t=0$, ν is the number of adsorbed segments, c_p is the polymer concentration, and D is the diffusion coefficient.

Equation 3.1 was derived by Lankveld (21) from the Ward Tordai equation (47). Details are given in Appendix V.

Some of the limiting assumptions in this equation are: (1) we assume diffusion of a low-molecular weight compound to a phase interface (with polymers this may refer to the adsorbing segments); (2) the equation does not consider adsorption to be finite and is, therefore, only valid during the initial phase of adsorption and at low concentrations; (3) we assume the two-dimensional equation of state, $\pi A = kT$, is applicable.

If diffusion was the limiting factor causing the time-dependency, then according to equation 3.1, γ_t vs $\sqrt{t}$ whould be linear at low PVA concentration during the initial phase of adsorption. The slopes of the lines, β_1, should increase with PVA concentration.

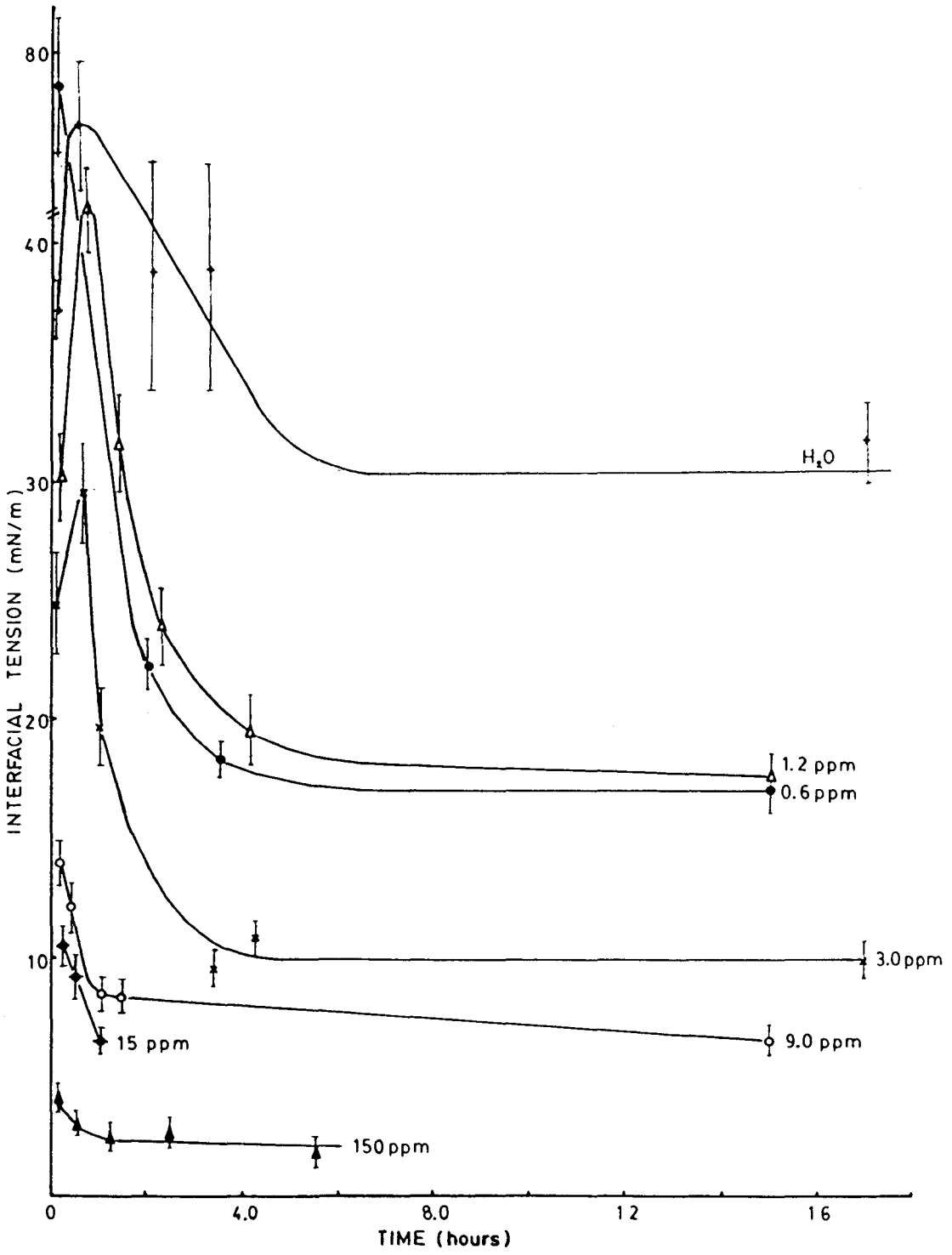

Figure 3.2 Interfacial tension between n-butyl chloride and PVA solutions as a function of time.

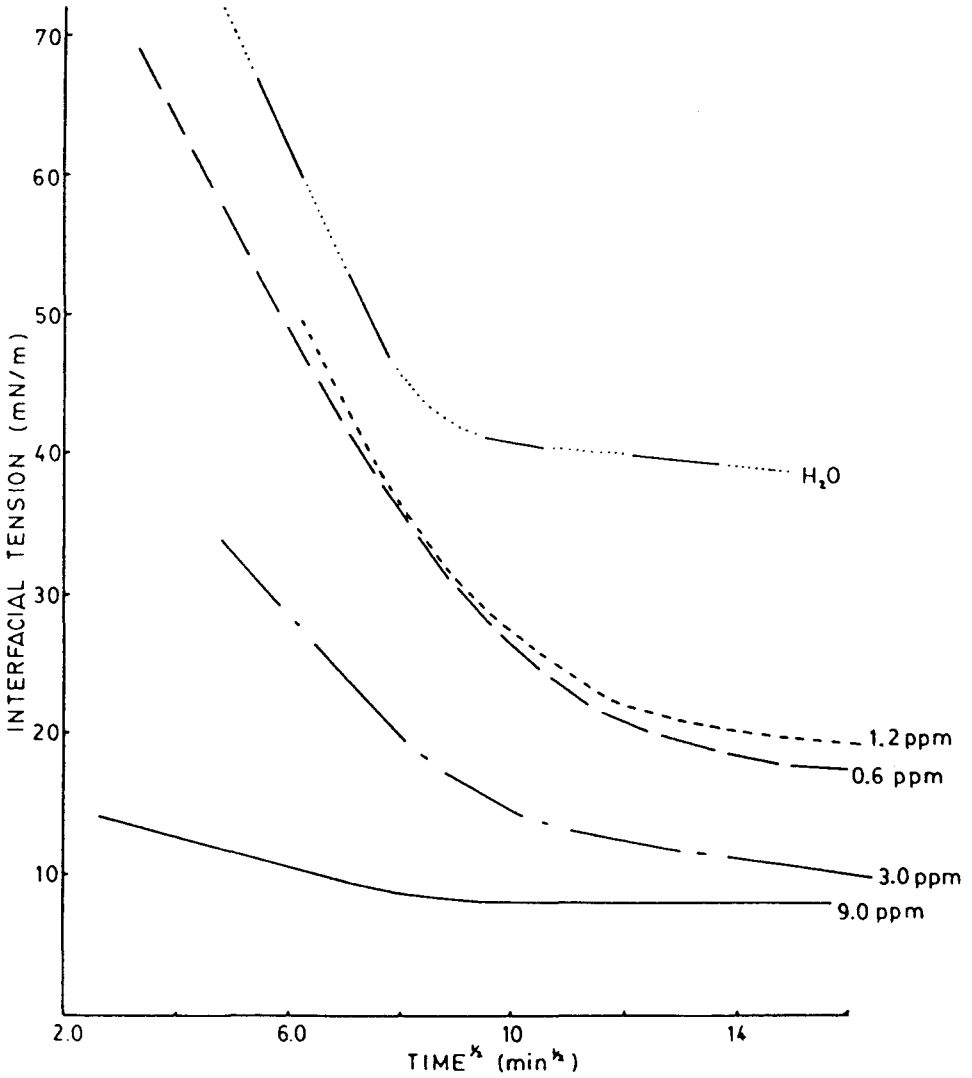

Figure 3.3 The interfacial tension between n-butyl chloride and PVA solutions as a function of time$^{1/2}$. Redrawn from the curves in Figure 3.2.

As seen in Figure 3.3 this does not seem to apply, although few data are available at lower concentrations and times less than five minutes. Perhaps the polymer-polymer interactions are such that this equation of state is not applicable and the concentration of adsorbing segments is therefore not easily related to the interfacial tension or, diffusion is not the major factor in the time-dependency. We conclude that reconformation of the interface layer is the prime reason for the time-dependency, although another possibility may be that there was contamination in the system of a small surface active molecule which was later displaced from the interface by the PVA polymer. Both these explanations are consistent with the fact that the pure water/n-butyl chloride interface also shows a time-dependency. Lankveld (21, p. 30) also recorded a drop in interfacial tension between water/paraffin of 1 mN/m in 8 hours.

Lankveld's (21) time studies showed little difference in the time-dependency between samples with different molecular weights but a marked difference between samples with different acetate contents. He found that for PVA with an acetate content, less than 2% and for low concentrations less than 2×10^{-4} g/dL (2 ppm), diffusion seemed to control the time-dependency. For PVA with an acetate content between 2% and 12% the time-dependency was explained by diffusion at low concentrations and reconformation at higher concentrations. However, there was no time study shown, or comment on their PVA with 23.5% acetate which would have been comparable to the PVA-KZ-04 in this study, which had an acetate content of 28%. Because of the highly hydrophobic character of the current PVA (high acetate content), it would be expected that diffusion would play a minor role in the time-dependency.

3.2 Steady-State Interfacial Tension and Polymer Adsorption

The steady-state interfacial tension measured between the PVA solution/n- butyl chloride as a function of concentration is shown in Figure 3.1 (curve c). In the concentration range studied, the interfacial tension decreased exponentially.

A problem often encountered in polymer adsorption is the irreversibility of the adsorption process. This implies that thermodynamic arguments cannot be used to describe equilibrium adsorption. Thus, the use of surface tension to yield surface concentration via the Gibbs adsorption isotherm equation is questioned by Lankveld (21). Yet, despite these questions Lankveld (21) combined Gibbs equation with the theories of Frish and Simha (15), and Katchalsky and Miller (20) to estimate the number of segments adsorbed per molecule, and the thickness of the adsorbed polymer layer respectively from $d\gamma/d\,\ell n\ c$ data by assuming a local equilibrium exists for the adsorption of individual segments. The equilibrium concentration is taken as the concentration of statistical chain elements in the subsurface. These, in turn, are correlated with the bulk concentration. Appendix VI lists these equations.

According to Lankveld's work (21), all the γ_t vs. c data with a concave shape (Figure 3.4, runs with PVA acetate content less than 2%) resulted in a decrease in the area per adsorbed unit and therefore a decrease in the number of segments adsorbed per molecule, and an increase in the adsorbed polymer layer thickness as the bulk polymer concentration increased. When a minimum area per unit of 0.3 nm^2 and a coordination number of 6 was used, this pseudo theory gave reasonable order of magnitude results. These values were later confirmed by indirect mass balance. Table 3.1 compares their results.

However, for polymers with higher acetate content, the shape of the γ vs. c curve was convex over most of the concentration range and, like this work for concentrations greater than 1.5×10^{-4} g/dL (Figure 3.1(c) and Table 3.2), the calculations predict an increase in the area per adsorbed unit for an increase in concentration. This is inconsistent with what

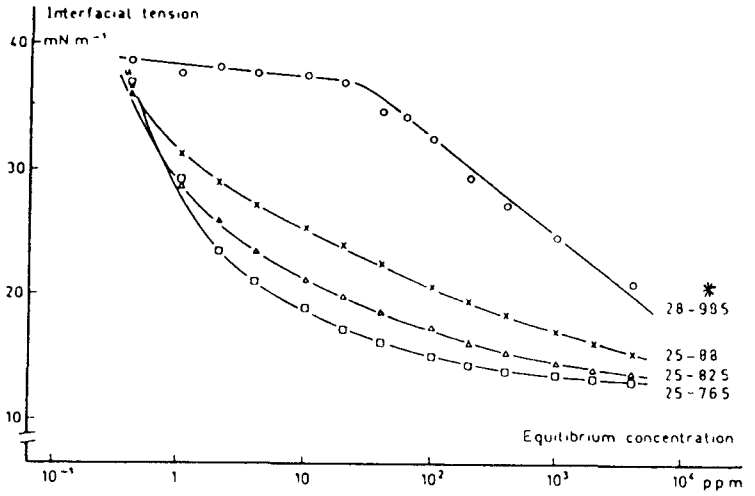

Figure 3.4. Influence of the acetate content of PVA ($\bar{P} \sim 1700$) on the interfacial tension. (21)
* refers to alcohol content (88 ≡ 12% acetate)

Table 3.1 Adsorption data derived from interfacial tension measurements (21)

1	2	3	4	5	6	7
Sample	$\bar{P}$	c_p (ppm)	β	$\frac{I}{\bar{\Gamma}}$(Å²)	ν	$\frac{\nu}{\bar{P}} \cdot 100$
8 - 98*	780	2 - 25	0.75	1240	124.0	15.9
		40 - 4000	4.65	200	20.0	2.6
16 - 98	1230	0.4 - 25	1.45	640	64.0	5.2
		40 - 4000	6.45	144	14.4	1.2
32 - 98	1780	0.4 - 25	2.05	454	45.4	2.6
		40 - 4000	6.95	134	13.4	0.8
3 - 98.5	290	0.4 - 10	1.15	810	81.0	27.9
		40 - 4000	7.85	118	11.8	4.1
28 - 98.5	1600	0.4 - 25	0.95	980	98.0	6.1
		60 - 4000	7.55	123	12.3	0.8
60 - 99	2340	0.4 - 25	1.75	530	53.0	2.3
		60 - 4000	7.65	122	12.2	0.5
105	535	0.4 - 10	1.25	744	74.4	13.9
		25 - 4000	4.05	298	29.8	4.3
124	2450	0.4 - 10	0.65	1430	143.0	5.8
		25 - 4000	3.40	274	27.4	1.1
4 - 88	450	4 - 4000	3.50	266	26.6	5.9
16 - 88	1220	4 - 4000	3.50	266	26.6	2.2
3 - 88	325	4 - 4000	4.25	218	21.8	6.7
25 - 88	1730	4 - 4000	3.95	236	23.6	1.4
40 - 88	2160	4 - 4000	4.10	227	22.7	1.1
25 - 82.5	1830	4	6.75	138	13.8	0.8
		100	3.60	258	25.8	1.4
25 - 76.5	1760	4	5.95	156	15.6	0.9
		100	3.50	266	26.6	1.5

β = slope of γ-log c_p curve

$\frac{I}{\bar{\Gamma}}$ = area per adsorbed unit according to GIBBS' law

ν = number of segments adsorbed per molecule according to FRISCH and SIMHA.

Table 3.2 PVA adsorption data calculated from interfacial tension measurements.

PVA Concentration (ppm)	β (mN/m)	$1/\Gamma$ ($\AA^2$)	ν	δ ($\AA$)
0.1 - 0.3	6.25	152	15.2	190
0.5 - 1.5	23.1	41.1	4.1	703
1.5 - 6.0	12.7	74.9	7.5	385
6.0 - 21	4.96	191	19.1	151
21 - 150	2.22	427	42.7	68

β = slope of γ - log c_p curve (Figure IV.1)

$1/\Gamma$ = area per adsorbed unit according to Gibbs' law

ν = number of segments adsorbed per molecule according to Frisch and Simha

δ = thickness of the adsorbed polymer layer (Eq. VI.3)

1ppm = 10^{-4} g/dL PVA

one would expect. Lankveld (21) had no explanation for this behaviour. The application of Gibbs equation in this case is therefore suspect and may only have meaning at very low concentrations (2, p. 3).

Hence, for the current system, the polymer adsorption data calculated from surface tension vs. bulk polymer concentration data are not viable values. However, we would expect the surface tension to decrease as more polymer adsorbs at the interface.

3.3 Film Thinning

When a butyl chloride drop was released from the capillary tip to the bulk interface the observed light interference patterns could be decomposed into five distinct mechanisms for the lamella behaviour according to Burrill (3). The mechanisms, observed by Burrill were 1) rapid approach of the drop to the interface, 2) dimple formation in the lamella, 3) slow even thinning, 4) uneven thinning, and 5) lamella rupture. A brief description of each mechanism will be presented below. Corresponding diagrams are found in Figure 3.5.

The mechanism of rapid approach is the simplest. Once a drop is released the drop buoyancy force causes the drop to accelerate to the bulk interface. Near the interface a lamella begins to form, and the decreasing thickness of the lamella begins to restrict flow. If an interfacial concentration of adsorbed polymer or surfactant is large enough, an interfacial tension gradient may be set up to balance the surface shear stress exerted on the interface. Both the drop buoyancy force and inertia force which acts on the drop as it decelerates do work on the bulk interface to set up this gradient. The drop buoyancy force is opposed by the lamella internal pressure, set up by the trapped fluid in the lamella. However, if there is insufficient polymer, both the drop and interface cannot support a shear stress. Both surfaces move radially outward, a relatively uniform lamella is seen, and the lamella thins rapidly to lamella rupture.

Figure 3.5 Mechanisms of lamella behaviour.

a) Lamella after dimple formation (a side view)

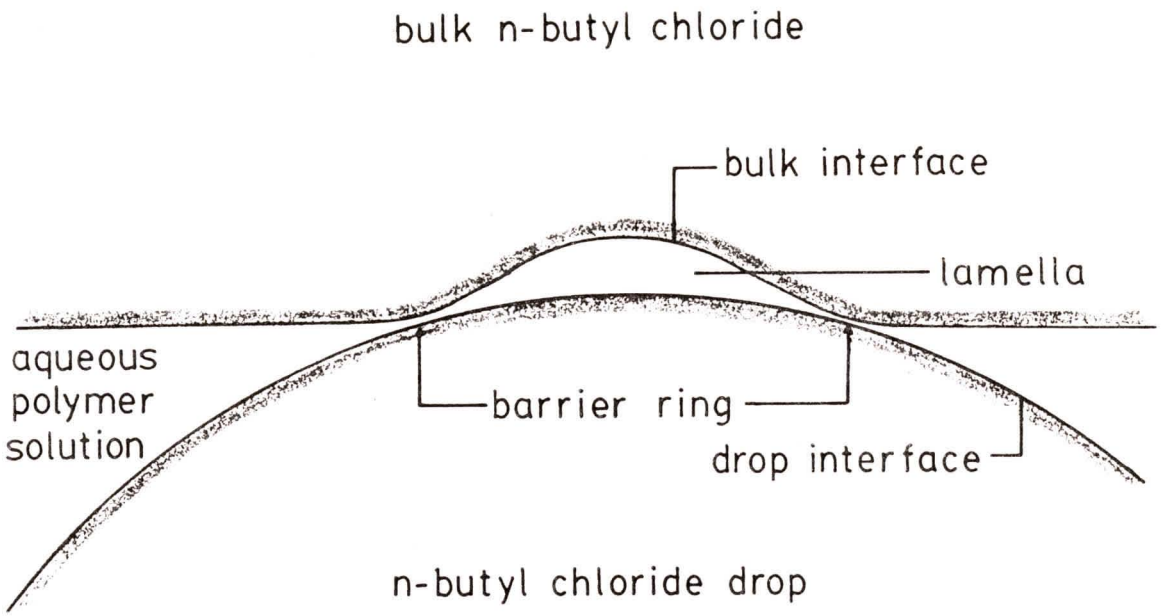

b) Photograph of even-thinning (a top view)

V=1.49 μL
T_R=8:15 min
PVA concentration
=3.11x10^{-4}g/dL
Magnification ~ 340x

c) Photograph of uneven-thinning (a top view)

V=2.78 μL

T_R=1:20 min

PVA concentration =62.0x10^{-4}g/dL

Magnification ~ 340x

d) Photograph of free energy wells just before rupture (top view)

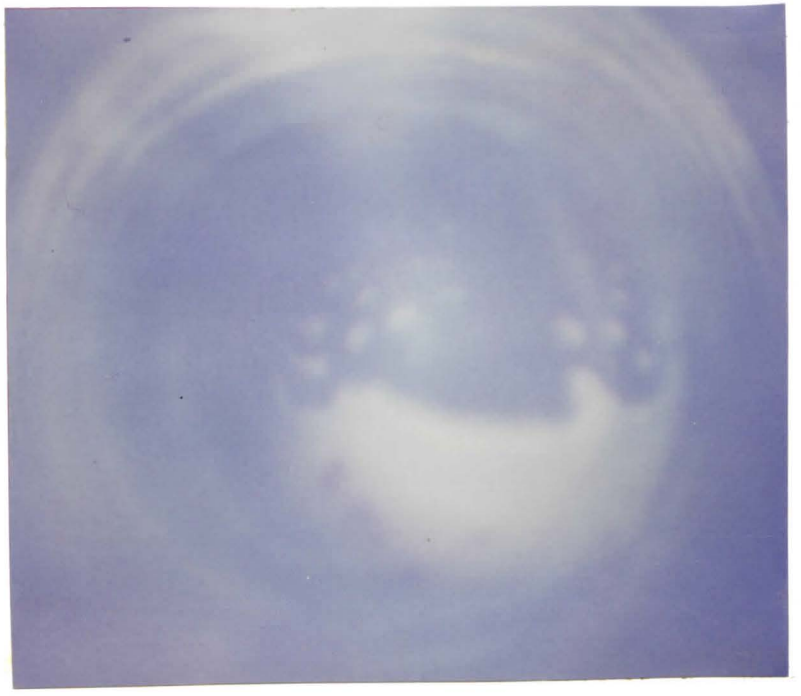

V=1.41 μL T_R=9:00 min
PVA concentration=0.0622 g/dL
Magnification ~ 490x

e) Photograph of local fluctuations in the lamella thickness (top view)

V=1.49 μL
T_R=21:30 min
PVA concentration=3.11×10^{-4} g/dL
Magnification ~ 340x

Once rapid approach has been completed, a large interfacial tension gradient may exist. This imbalance causes the bulk interface to contract carrying fluid inward, thus reducing the interfacial tension gradient to balance with the surface shear stress. In this way a dimple is formed, increasing the thickness of the lamella at its centre. Dimple formation was never seen in this study, since interference patterns were only recorded once thinning had begun. A diagram of the lamella at this stage is shown in Figure 3.5(a).

During slow even thinning, Figure 3.5(b), there was a slow contraction of the bulk interface because there was a decrease in the surface shear stress with a decrease in the overall lamella thickness.

During uneven thinning, the contents of the dimpled region of the lamella flows preferentially out of one side of the barrier ring. The overall lamella thickness decreases rapidly to give an almost constant lamella thickness with radius, and lamella thinning becoming very slow. Figure 3.5(c) illustrates this mechanism. In the present study this type of lamella drainage was observed for polymer concentrations greater than 3.11×10^{-4} g/dL. With a polymer concentration of 3.11×10^{-4} g/dL, even thinning was observed and rupture usually occurred within two minutes. Often drops were observed to move at the interface in a direction opposite the drainage point.

The usual drainage pattern observed by Van Vliet (44) with his held films was similar to this work. The film initially drained with a dimple. When the dimple disappeared the films were parallel and homogeneous and the drainage became very slow.

Rupture of the lamella occurred when the light interference pattern was either grey or black (40 - 20 nm). For aqueous polymer concentrations less than 0.03 g/dL rupture occurred in the grey region. At the higher polymer concentrations black spots appeared on the grey interference pattern just before rupture. This observation was also reported by Frankel and Mysels (14) and interpreted by Princen and Mason (31). The lamella falls into a

free energy minimum which implies there must be some repulsion. A photograph of this phenomena is presented in Figure 3.5(d).

Several explanations have been suggested for the cause of rupture at these thicknesses, such as dirt, vibrations, macroscopic and statistical thermal fluctuations which cause interfacial tension gradients, van der Waals forces and Brownian motion. Our experimental set up eliminated dirt, vibrations, and macroscopic thermal fluctuations as possible causes. De Vries (6) had calculated that the magnitude of statistical thermal fluctuations was too small to cause rupture.

Van der Waals forces increase gradually as the lamella thickness is decreased, and are often incorporated into lamella drainage models (Hodgson and Woods (18), MacKay and Mason (25), Vrij and Overbeek (46)). Thus, van der Waals attractive force and local thickness fluctuations are considered to be the causes of lamella rupture between 40-20 nm.

Local fluctuations in the lamella thickness (Figure 3.5(e)) were observed occasionally at higher polymer concentrations and/or interface ages.

By varying the polymer concentration in the aqueous phase we observed an effect on the lamella thinning. This effect is represented in Figures 3.6 and 3.7 by plotting the average thickness of the lamella from the time the drop was released to the bulk interface. Table 3.3 lists the coalescence times with respect to the polymer concentration. From Figure 3.6 and Table 3.3 we find: 1) films stabilized with 3.11×10^{-4} g/dL (3.11 ppm) PVA generally coalesced within two minutes. 2) films stabilized with 62×10^{-4}g/dL (62 ppm) PVA were generally stable at an average film thickness of approximately 100 nm. 3) films stabilized with 620×10^{-4} g/dL and 310×10^{-4} g/dL PVA coalesced within approximately ten minutes. 4) the time elapsed from surface cleaning to drop release had no effect on the thinning rate. Van Vliet (44) found that a reduction in the waiting time, before bringing the two surfaces together, from one hour to two minutes did not influence the equilibrium thickness. He

proposed that the reconformation of the adsorbed PVA may lead to a measurable change in interfacial tension but not to a measurable change in steric repulsion.

Figure 3.7 represents experiments performed with n-butyl chloride (Baker Analyzed) which contained less impurities than that used in Figure 3.6. Impurities in the system seemed to affect the film thinning. The lamella formed with the 300 ppm PVA and Baker Analyzed n-butyl chloride was of a greater thickness than that formed with the TM reagent grade n-butyl chloride. Indeed, 300 ppm PVA with Baker Analyzed n-butyl chloride gave data more like 62 ppm PVA with TM n-butyl chloride. One might attempt to compare these by estimating an average (over the drop diameter) "steady-state" thickness for each concentration of PVA added and compare these for the two grades of n-butyl chloride. The results are shown in Figure 3.8. The average "steady-state" film thickness for the systems containing more impurities (TM grade n-butyl chloride) was less than that for the cleaner Baker Analyzed n-butyl chloride. The presence of impurities reduced the film thickness. Some of the impurities were found experimentally to be water soluble and ionic in nature. The presence of the impurities may have changed the affinity of the polymer for the n-butyl chloride and/or the conformation of the polymer at the n-butyl chloride/H_2O interface.

Let us now consider the systems containing the TM reagent grade n-butyl chloride. All further discussion will be concerned with these systems, unless otherwise stated.

If we assumed, in general terms, that the interfacial tension was a measure of the excess polymer segment concentration, then according to Figure 3.1(c), when the polymer concentration was greater than 15×10^{-4} g/dL, the interface was likely saturated with polymer segments. Thus we can reason that with a polymer concentration of 3.11×10^{-4} g/dL the interface was likely not saturated so there was very little resistance to lamella thinning and

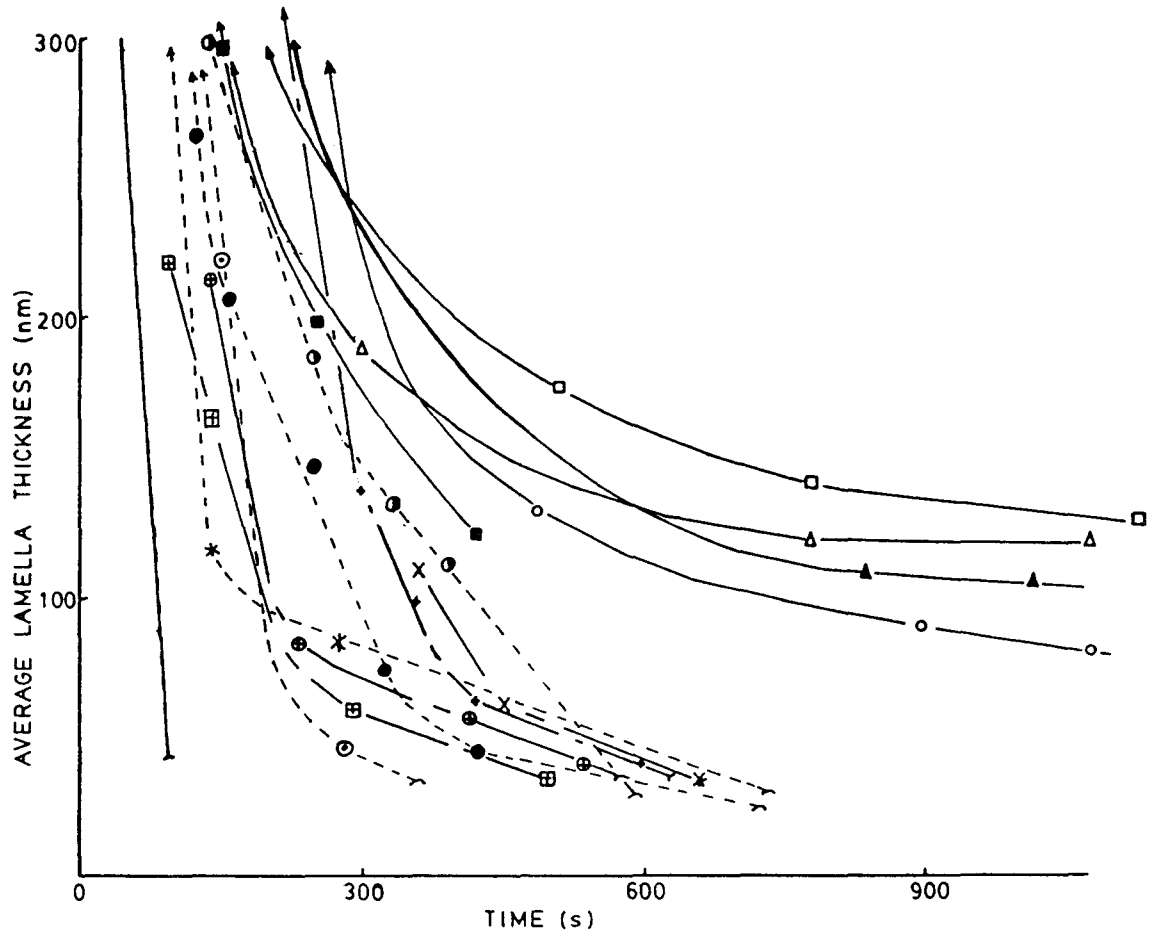

Figure 3.6 Average lamella thickness as a function of time from drop release. ($\wedge$ =coalescence point)

PVA Concentration (ppm)	Drop Volume (μL)	Symbol
3.11	1.58 to 1.98	——
62.0	1.00	o
	1.17	□
	1.33 & 1.42	△
	1.74	▲
	2.78	■
310	2.46	⊙
	0.64	*
	1.90	●
	3.02	◑
620	1.41	⊕
	3.42	+
	1.49	×
	1.01	⊞

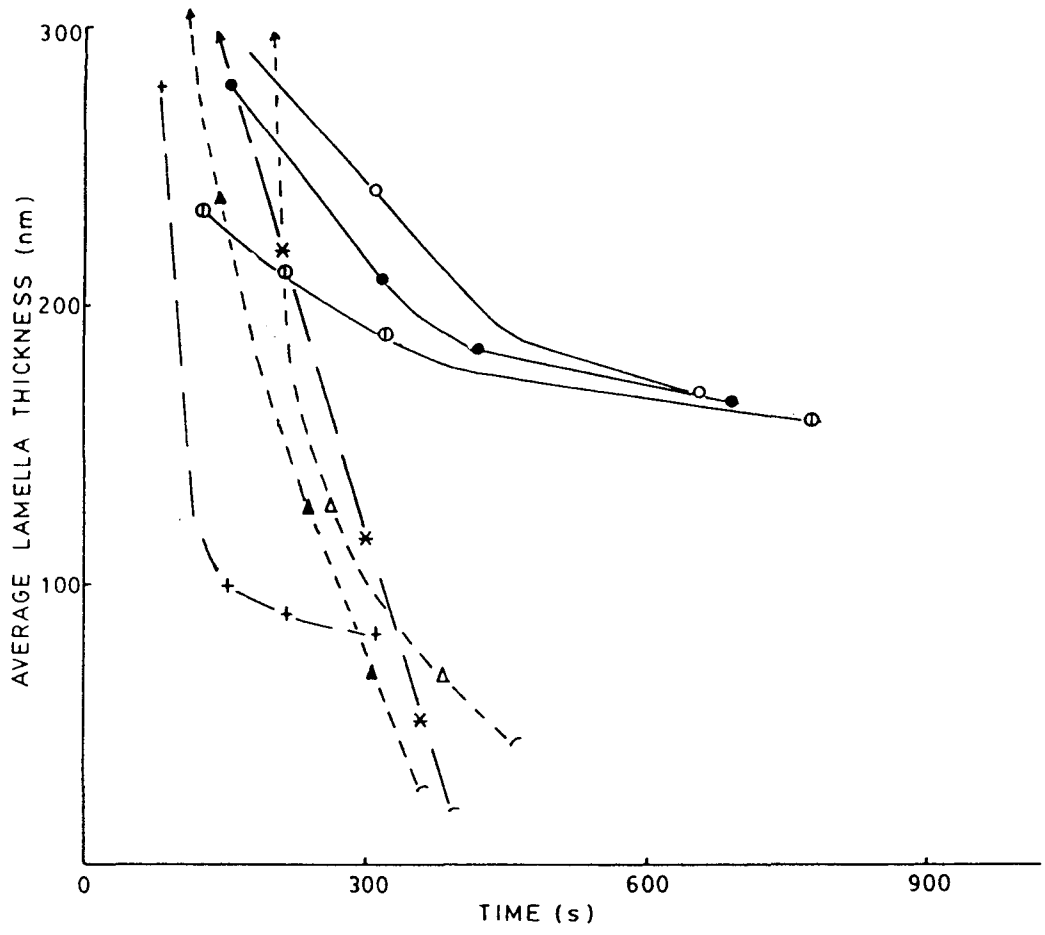

Figure 3.7 Average lamella thickness as a function of time from drop release. (n-butyl chloride - Baker Analyzed)

PVA Concentration (ppm)	Drop Volume (μL)	Symbol
300	2.13	●
	1.40	Φ
	2.45	o
600	1.00	+
	3.58	*
1200	2.05	▲
	3.42	Δ

⌒ =coalescence point

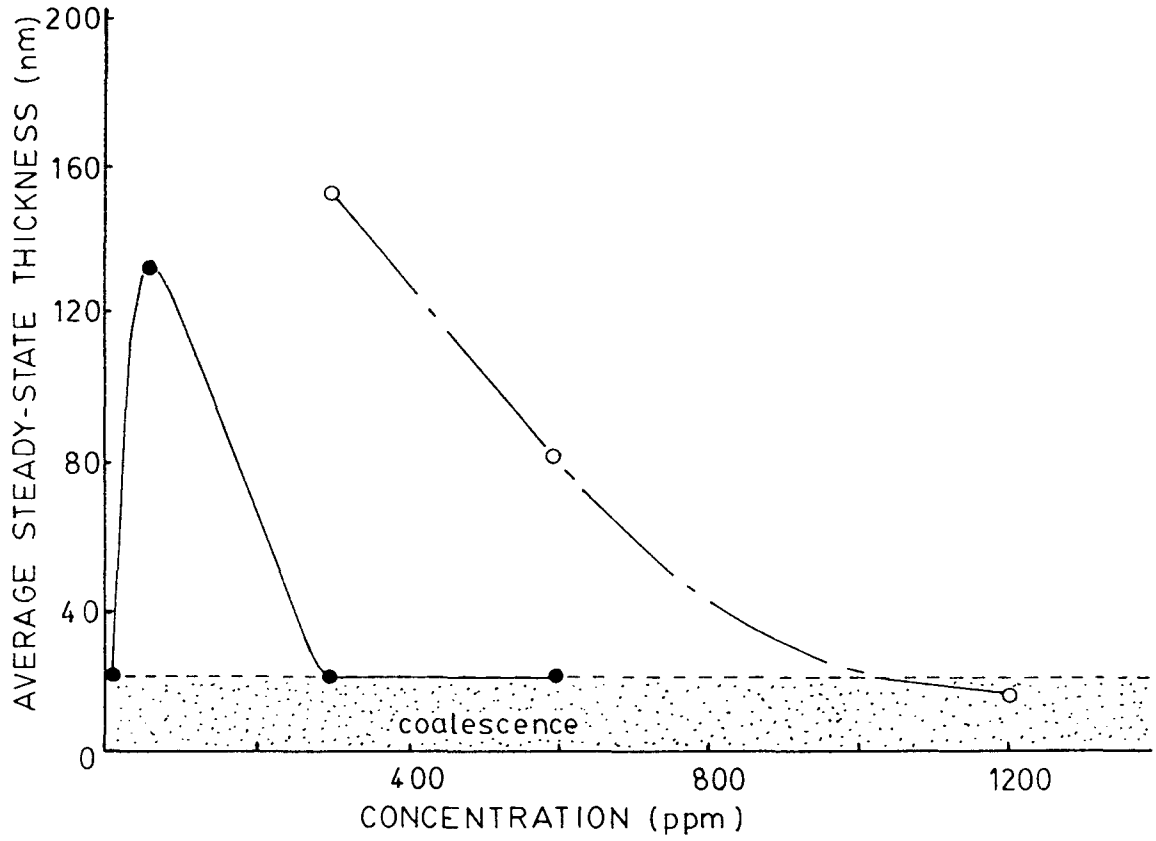

Figure 3.8 The average steady-state film thickness as a function of PVA concentration. ● Baker TM reagent grade n-butyl chloride, ○ Baker Analyzed n-butyl chloride.

Table 3.3 Coalescence time with respect to polymer concentration *

Polymer Concentration (g/dL)	V μL	T_S hr:min	T_E min:s	T_R min:s
3.11×10^{-4}	1.58	9:05	0:28	1:30
	1.75		0:12	2:00
	1.98	9:39	0:35	0:20
0.00620	1.00	2:16	0:33	still there after 47:00
	1.09		0:29	still there after 30:00
	1.17	5:31	0:11	still there after 60:11
	1.33	7:50	0:04	still there after 24:18
	1.42	6:53	0:10	still there after 27:30
	1.74	4:38	0:20	30:00
0.0622	1.01	3:21	0:34	8:20
	1.41	0:34	0:01	10:45
	1.49	0:12	0:04	3:45
	1.49	1:33	0:24	10:40
	1.74	2:10	0:51	10:20

Table 3.3 continued

Polymer Concentration (g/dL)	V μL	T_S hr:min	T_E min:s	T_R min:s
	3.42	0:54	0:05	10:30
0.031	0.64	1:44	0:32	12:00
	1.90	0:36	0:06	12:40
	2.46	0:18	0:07	5:45
	3.02	1:23	0:03	9:50
	3.58	2:31	0:30	10:45

V = drop volume ($\mu L \pm 0.05$ L)

T_S= time elapsed from initial surface formation to drop release

T_E= time elapsed from surface cleaning to drop release

T_R = time elapsed from time of drop release to coalescence

* = TM reagent grade n-butyl chloride

the drop coalesced within two minutes. All the other concentrations studied were greater than $15x10^{-4}$ g/dL and therefore possessed a saturated interface.

Why then should the drops in the system with polymer concentration of 0.0062 g/dL have the slowest lamella thinning rate? Other researchers have also found such behaviour. For example Li-In-On, Vincent, and Waite (24) found there was a critical concentration for poly (ethylene oxide) stabilized latex dispersions above which stability decreased.

In our study, the systems interfacial tensions and densities were approximately the same for concentrations greater than $15x10^{-4}$ g/dL, only the number of polymer particles in the bulk had increased. As can be seen from the interfacial tension data this hydrophobic PVA polymer is very surface active and perhaps at the higher concentrations, the lower molar mass fraction of the molar mass distribution diffused more rapidly to the surface thus causing the thickness of the adsorbed layer to be smaller, which may have reduced the steric repulsion and thus caused a faster rate of thinning. This, however, seems unlikely since at higher polymer concentrations diffusion would be less important than at lower concentrations. Perhaps what happened, then, was that as the polymer concentration increased the amount of PVA polymer adsorbed onto the butyl chloride surface increased, keeping the number of segments adsorbed about the same, but increasing the polymer extension into solution. The thickness of the polymer layer was therefore increased. During lamella thinning the polymer- polymer interaction, which tended to be attractive due to the hydrophobic character of the polymer occurred at a larger film thickness and therefore sooner than for the lower concentration of 0.0062 g/dL.

This can be explained in terms of the HVO steric stabilization model. The total free energy change for the approach of two flat plates with sufficient polymer coverage is

$$\Delta F_T = \Delta F_{VR} + \Delta F_M + \Delta F_A$$

$$\Delta F_T = 2\nu\, kT\, V(\tau,d) + 2\left(\frac{2\pi}{9}\right)^{3/2} \nu^2\, kT(\alpha^2 - 1)(i\,\ell^2)\, M(\tau,d) - \frac{A}{12\,\pi\, d^2} \qquad [3.2]$$

When ΔF_T is positive at all distances of separation we have repulsion and thus stability against coagulation. If α, the dispersion medium - polymer affinity or chain expansion parameter, is less than one (an unfavorable dispersion medium) then ΔF_M is negative. Also as the number of adsorbed loops or tails per unit surface area, ν, which is related to the polymer concentration in solution, increases then ΔF_{VR} increases linearly with the amount of polymer adsorbed whereas ΔF_M increases with the square.

Meier (27) compared the contribution of ΔF_M to that of ΔF_{VR} and found that for small surface coverage $\Delta F_M << \Delta F_{VR}$ whereas for large surface coverage ΔF_M is comparable to ΔF_{VR} at long separations.

Figure 1.4 shows the theoretical dependence of stability on the quality of the dispersion medium, α, and the amount of polymer adsorbed ω. To the right of each curve the system is stable against coalescence and to the left it is unstable. These curves are examples of some of the possible systems which may exist. According to the explanation given above the PVA polymer/H_2O system in this study would have been similar to the system represented by curve (b): unstable when the polymer concentration was low, 3.11×10^{-4} g/dL, stable near the polymer concentration of 0.006 g/dL and unstable when the polymer concentration was about 0.03 g/dL or greater.

If we assume that impurities change the quality of the solvent, then according to Figure 1.4, curve (b) by decreasing α slightly, an amount of polymer which previously caused stability is now shifted toward the unstable region. This was experimentally observed for the 300 ppm PVA concentration. (See Figures 3.6, 3.7 and 3.8.)

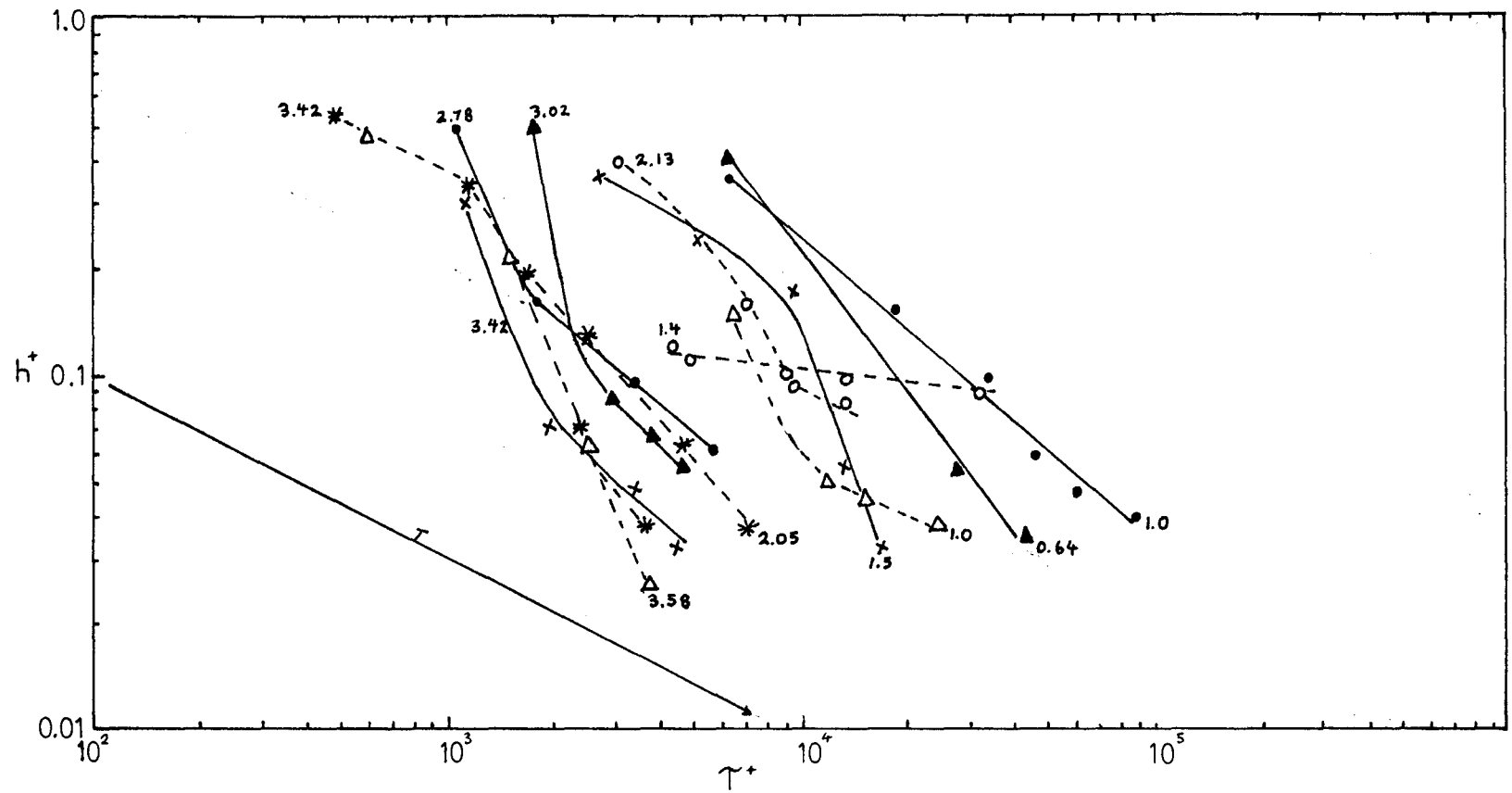

Figure 3.9 Dimensionless thickness (h^+) as a function of dimensionless time (τ^+) for the modified parallel disc model. Theoretical vs experimental values for various drop volumes and PVA concentrations.

TM reagent grade n-butyl chloride: • 62.0 ppm, ▲ 310 ppm, × 620 ppm
Baker Analyzed n-butyl chloride: o 300 ppm, △ 600 ppm, * 1200ppm
Theoretical curve: ___1___

Van Vliet (44) measured the equilibrium thicknesses and rates of thinning of PVA stabilized held films as a function of hydrostatic suction over the film. He found only a very small difference between the 400 ppm and 4000 ppm solution, but a very strong influence of molecular weight. He was also able to construct a potential energy curve from his results since for his system $f_A + f_H + f_S = 0$ where $f_A = A_{11}/6\,\pi\,h_f^3$ is the attractive force, $f_H = -\Delta\rho g/\ell$ is the hydrostatic suction force, and f_S is the steric repulsion force. The variables h_f and ℓ were measured at steady state. Thus f_s was calculated. Then by numerically integrating the $f_s(h)$ curve be obtained the potential energy curve. When he compared his experimental curve with the HVO calculated curve he found good agreement with a 'most probable' molecular weight distribution and considering a fixed percentage of the segments adsorbed in the one or two tails per molecule. In his system a few long tails dominated the properties of the outer part of the adsorbed polymer layer.

A steric repulsion force curve, $f_s(h)$, could not be constructed with the results from this thesis because only one point on the potential energy curve could be calculated. Only the films obtained using 0.00622 g/dL PVA reached steady state and that would only give one point on the curve.

Although the focus of this research is 'stable equilibrium' films, data were taken to show the rate of approach to equilibrium or the rate of film thinning. Thus, the thinning data can be used to help us understand more about the coalescence process for drops stabilized by polymer. Various models have been proposed to describe the rate of film thinning of drops stabilized by surfactants. A modified parallel disc model has been proposed by Liem and Woods (23) of the form

$$\tau^+ = \left(\frac{1}{h^+}\right)^2 - 1 \qquad [3.3]$$

where τ^+ is dimensionless time

$$\tau^{+} = \frac{16}{4\phi}\left[\frac{\gamma^2}{\mu_c \Delta\rho\, g}\right]\frac{1}{b^3}\left(\frac{h_1}{b}\right)^2 \tau \qquad (3.4)$$

γ is the surface tension (44 mN/m), u_c is the viscosity of the continuous phase in the film (1.00 cp), $\Delta\rho$ is the density difference (0.114 g/mL), g is the acceleration due to gravity, b is the radius of the drop, h_1 is the initial thickness of the film immediately after release from the nozzle (assume 2000 nm), ϕ is a function that varies depending on the local mobility, $\phi = (4-2n_m)/(1+n_m)$ and n_m is the number of locally mobile surfaces ranging from 0 to 2.

The data in Figures 3.6 and 3.7 show data for different drop volumes. These can be standardized to one basic curve if all the thinning follows the same fluid dynamic pattern and if the correct dependency of thinning rate on drop diameter can be found. Figure 3.9 shows the data from Figures 3.6 and 3.7 compared with the modified parallel discs model ($\phi=4$). Because the current data are average film thicknesses, one must be careful not to read to much into the data. This model does not seem to account correctly for the diameter dependency and there is a concentration dependence in the data not accounted for in the model. Further work should be conducted on this coalescence theory as it applies to drops stabilized by polymers. Despite the weakness of the coalescence model, one interesting feature emerges. The theory used assumed that both surfaces had no mobility; that is, that they behaved as rigid surfaces. Data lying to the left of the theory would be described as having "some mobility"; this would be accounted for through the local mobility factor ϕ. However, data lying to the right of the theoretical line cannot have more than both surfaces rigid. What this suggests is that the presence of the polymer must increase the effective viscosity of the fluid trapped between the surfaces.

3.4 Emulsions Stabilized by PVA

Bohm (2) suggests that the behaviour of polymers at undisturbed interfaces cannot be directly compared with the behaviour at disturbed interfaces. However, because it was known that industrial polymerizations often used stabilizing polymers at concentrations of about 0.06 g/dL and the thin film experiments showed coalescence at this concentration, qualitative emulsion experiments were performed to observe the degree of dispersion and coalescence in emulsions of butyl chloride drops stabilized with 0.006 g/dL, 0.03 g/dL, and 0.06 g/dL of PVA.

Once solution mixing was complete, the drops that were formed in the 0.006 g/dL PVA solution coalesced into larger drops such that the average drop volume was larger than the drop volume observed with the 0.03 g/dL PVA and 0.06 g/dL PVA.

After the emulsion layer separated from the aqueous layer, the number of drops per unit volume of butyl chloride was much less with the 0.006 g/dL PVA solution than with the 0.03 g/dL PVA and 0.06 g/dL PVA solutions. For the latter two concentrations, the degree of dispersion was indistinguishable and the emulsion was extremely stable.

We attribute the observed difference between the lower PVA concentration, 0.006 g/dL, and the two higher concentrations to the number of polymer particles available to form stable drops with the increased surface area upon mixing.

If we assume our system can be represented by curve (b) in Figure 1.4, then at the lower concentration, because of the large increase in surface area, the amount of polymer adsorbed per cm^2 just after mixing brings us below the curve into the unstable region. After some coalescence has taken place to the point where the amount of polymer adsorbed per cm^2 has increased, because the surface area has decreased, to an amount just above the curve. Now, the drops are stable but larger in volume. At the two higher concentrations (0.03 g/dL and 0.06 g/dL PVA) just after mixing, the amount of polymer adsorbed per cm^2 is enough to

produce stable drops and no coalescence was observed. If this explanation is correct and therefore consistent with the film thinning experiments, if we continue to increase the concentration of the polymer in the aqueous phase, we should reach a point where we will again be in the unstable region and the degree of dispersion should decrease, unless we reach the limits of solubility first. This type of behaviour has been observed by Lankveld (21) with heptane-water emulsions stabilized by PVA (12% acetate) in the concentration range 10 ppm PVA to 2000 ppm PVA.

Estimates can be made to establish how much polymer is needed to saturate a given amount of area. Lankveld (21) and Fleer et al. (48) determined in emulsion experiments that in general: 1) the maximum amount of polymer adsorbed is between 2.0 - 4.5 mg/m^2. 2) About 80% of the surface is covered with trains of polymer. 3) about 10% of the polymer segments reside as trains. 4) each segment occupies between 0.15 nm^2 and 0.30 nm^2. Based on these data and assuming that all the polymer adsorbed so that the amount in solution was negligible, then for PVA-KZ-04 of molar mass 23,300 and a degree of polymerization of 400, the area covered per litre is given in Table 3.4.

For an emulsion of 50% v/v PVA solution and n-butyl chloride with drops approximately 50 µm in diameter the area would be about 120 m^2/L, which is about 1500 times larger than the cell area used in the thin film experiments. Thus, according to Table 3.4, this area would require about 300 ppm (0.03 g/dL) of polymer to saturate the surface. The average drop diameter was not experimentally determined in the present work, therefore this calculation is only speculative.

Table 3.4 Estimated surface area that can be saturated by polymer.

Polymer Concentration (ppm)	Estimated Maximum area that can be saturated	
	Method 1 (m^2/L)	Method 2 (m^2/L)
3.11	1.2	0.7 to 1.5
62	24	14 to 31
300	115	67 to 150
600	230	135 to 300
1200	465	270 to 600

Method 1: (eg. 62ppm)

$$\left(62\times10^{-3}\frac{g}{L}\right)\left(\frac{1\text{ mole}}{23{,}300\text{ g}}\right)\left(6.023\times10^{23}\frac{\text{molecules}}{\text{mole}}\right)\left(\frac{400\text{ seg.}}{\text{molecule}}\right)\left(\frac{0.1}{0.8}\right)$$

$$*\left(0.3\times10^{-18}\frac{m^2}{\text{seg.}}\right)= \quad 24\ m^2/L$$

Method 2:

Assume 2 to 4.5 mg/m^2 of polymer is adsorbed.

CHAPTER 4

CONCLUSIONS

The Hodgson and Woods method (18) used in this work to study thin films provided an easy way to form free thin films stabilized by PVA and since in real life free films are more often encountered rather than held films, this method was a more realistic probe to study polymer stabilized thin films than van Vliet's method (44), even though the van Vliet measurements were more accurate. However, the method used in this study could not be used to obtain a potential energy curve for the system as was van Vliet's method because only one steady state point could ever be obtained on any curve. An added complication to the Hodgson and Woods method was the buoyancy effect which introduced an added force. If we could relate the coalescence time to stability (or ΔF_{min}) of emulsions then this method could be a useful tool to determine the stabilizing ability of a polymer.

Vibrations from the building which manifested themselves at the bulk n- butyl chloride/PVA solution interface as waves caused drop migration and had to be eliminated by mounting the equipment onto a cement block which rested on rubber pads.

The observed lamella thinning patterns have all been previously observed by Burrill (3). An uneven drainage pattern was observed for all concentrations except 3.11×10^{-4} g/dL. Fast dimple drainage and then slow thinning was also observed by van Vliet (44). Film rupture was observed for the PVA concentrations of 3.11×10^{-4} g/dL, 0.0622 g/dL and 0.031 g/dL. For some of the films at the higher concentrations of 0.0622 g/dL and 0.031 g/dL, the lamella fell into a free energy well and black spotting occurred just before rupture. With the less contaminated n-butyl chloride, film rupture was not observed with the 0.030 g/dL PVA within the 13 minute observation time, and the film was thicker than was observed with the more contaminated reagent grade n-butyl chloride. Film rupture was observed with the 0.06g/dL and 0.1200 g/dL PVA.

The time elapsed from surface cleaning to drop release to the bulk interface had no effect on the rate of thinning. A similar finding was observed by van Vliet (44) who postulated that the reconformation of the adsorbed PVA may lead to a measurable change in the interfacial tension but does not seem to affect the lamella thinning and thus the steric repulsion.

Attempts to relate the lamella thinning rate and drop size dependency to a coalescence theory was encouraging but not successful. More theoretical work is required in this area, although the data suggests that the adsorbed polymer increases the local effective viscosity.

The reagent grade n-butyl chloride drop coalesced within two minutes when the concentration of the stabilizing PVA was 3.11×10^{-6} g/dL. The drop was observed to be stable when the concentration of PVA was 0.0062 g/dL and then coalesced when the concentration of PVA was raised to 0.062 g/dL and 0.031 g/dL. The stability (ΔF_{min}) decreased at the higher PVA concentrations possibly due to an increase in film thickness at which the two adsorbed layers start to interact, thus according to the HVO theory, the free energy of mixing, ΔF_M, becomes important and because of the hydrophobic character of the PVA (28% acetate) the mixing term will tend to increase the attraction. This attraction is not observed when 0.0062 g/dL PVA is used as stabilizer because, with the resulting surface coverage, $\Delta F_{VR} > \Delta F_M$ at the point of interaction. Van Vliet observed only a small effect on the held film thickness when comparing films stabilized by 400 ppm and 4000 ppm PVA solutions. Both these concentrations could be considered at the high end of our concentration range. When cleaner n-butyl chloride was used, the average "steady-state" film thickness was larger than the film thickness observed for the TM reagent grade n-butyl chloride. The impurities present in the TM grade may have changed the solvent quality, causing a change in the polymer affinity for the n-butyl chloride and/or a change in the polymer conformation at the interface.

The trends observed in this work were explained by the HVO theory. Current theories require many variables; solvent power, polymer surface coverage, polymer conformation, polymer molecular weight distribution, which are often difficult to assess.

Results obtained from the thin film experiments could not be directly related to emulsions, in part because of the great difference in surface area. From our thin film experiments we could predict trends. A maximum in stability (when ΔF_{min} is minimized) should occur with increasing PVA concentration. Lankveld (21) observed this type of behaviour with heptane-water emulsions stabilized by PVA (12% acetate). Our suspensions were stable with 50% n-butyl chloride and PVA solutions with concentrations of 0.03 g/dL and 0.06 g/dL.

The drop weight method of determining interfacial tension could not be used to determine the interfacial tension between n-butyl chloride and PVA solutions. Because the interface was constantly expanding with this method ,a new surface was exposed at which the PVA macromolecule could adsorb and steady-state was never reached before the drop fell. Both the Wilhelmy plate and spinning drop method were appropriate for determining the interfacial tension given the interface had enough time to reach steady-state. Five hours was sufficient time for the spinning drop method. Lankveld (21) allowed the interface to stand between 18 and 30 hours before using the Wilhelmy plate to determine the steady-state interfacial tension.

The interfacial tension between n-butyl chloride and PVA solutions decreased with time from moment of interface formation to reaching steady-state. Lankveld (21) found that for low concentrations of PVA (2% to 12% acetate), less than 2.0 ppm, the time-dependency of the interfacial tension could be explained by diffusion. At higher concentrations he attributed the time- dependency to polymer reconformation. In this study the time-dependency of the PVA (28% acetate)/n-butyl chloride interfacial tension for the PVA

concentration range 0.6 ppm to 150 ppm could not be explained by diffusion and was therefore attributed to polymer reconformation.

The steady-state interfacial tension between a PVA solution and n-butyl chloride decreased exponentially with increasing PVA concentration from 32 mN/m at zero PVA.

The steady-state interfacial tension could not be related to the excess PVA polymer concentration at the PVA/n-butyl chloride interface by the Gibbs' adsorption isotherm equation because of the irreversibility of the polymer adsorption. Attempts to consider the segments of the polymer as the reversible species, as did Lankveld (21), did not produce reasonable results in the concentration range studied. The interfacial excess polymer concentration was therefore not calculated.

The interfacial tension measurements on the PVA/n-butyl chloride system provided the following information: 1) polymer reconformation at the interface lowers the interfacial tension as does the excess interfacial polymer segment concentration. 2) Gibbs' isotherm equation could not be applied to the system studied due to the irreversibility of the polymer adsorption.

APPENDIX I

Determination of Intrinsic Viscosity and Root-Mean-Square End-to-End Distance of Polymer PVA-KZ-04

The PVA-KZ-04 solutions were prepared from a stock 0.836 g/dL solution. Five millilitres of solution were placed in an Ostwald viscometer set in a 25 ± 0.5°C thermostatically controlled water bath. The specific viscosity of the solution was calculated from the measured values of the flow time and density.

According to equation I-1, the intrinsic viscosity of a polymer can be determined by an extrapolation to infinite dilution (19)

$$[\eta] = \lim_{c \to o} \frac{\eta - \eta_s}{\eta_s c} = \lim_{c \to o} \frac{\eta_{sp}}{c} \qquad [I.1]$$

where $[\eta]$ is the intrinsic viscosity, η is the solution viscosity, η_s is the solvent viscosity, and c is the solution concentration. Thus for PVA-KZ-04 $[\eta] = 0.229$ dL/g at 25°C (Figure I.1).

The root-mean-square end-to-end distance, $(\overline{r^2})^{\frac{1}{2}}$, of this polymer at 25°C is determined by (11)

$$[\eta] = \frac{\phi (\overline{r^2})^{3/2}}{\overline{M}_v} \qquad [I.2]$$

where $\phi = 2.1 \times 10^{21}$ (44) and $\overline{M}_v$ is the viscosity average molecular weight, 23,300 (34). The value of $(\overline{r^2})^{\frac{1}{2}} = 13.6$ nm, and is in agreement with the values obtained by Van Vliet (44) for a similar system.

Figure I.1 Evaluation of the intrinsic viscosity of PVA-KZ-04 in water at 25°C.

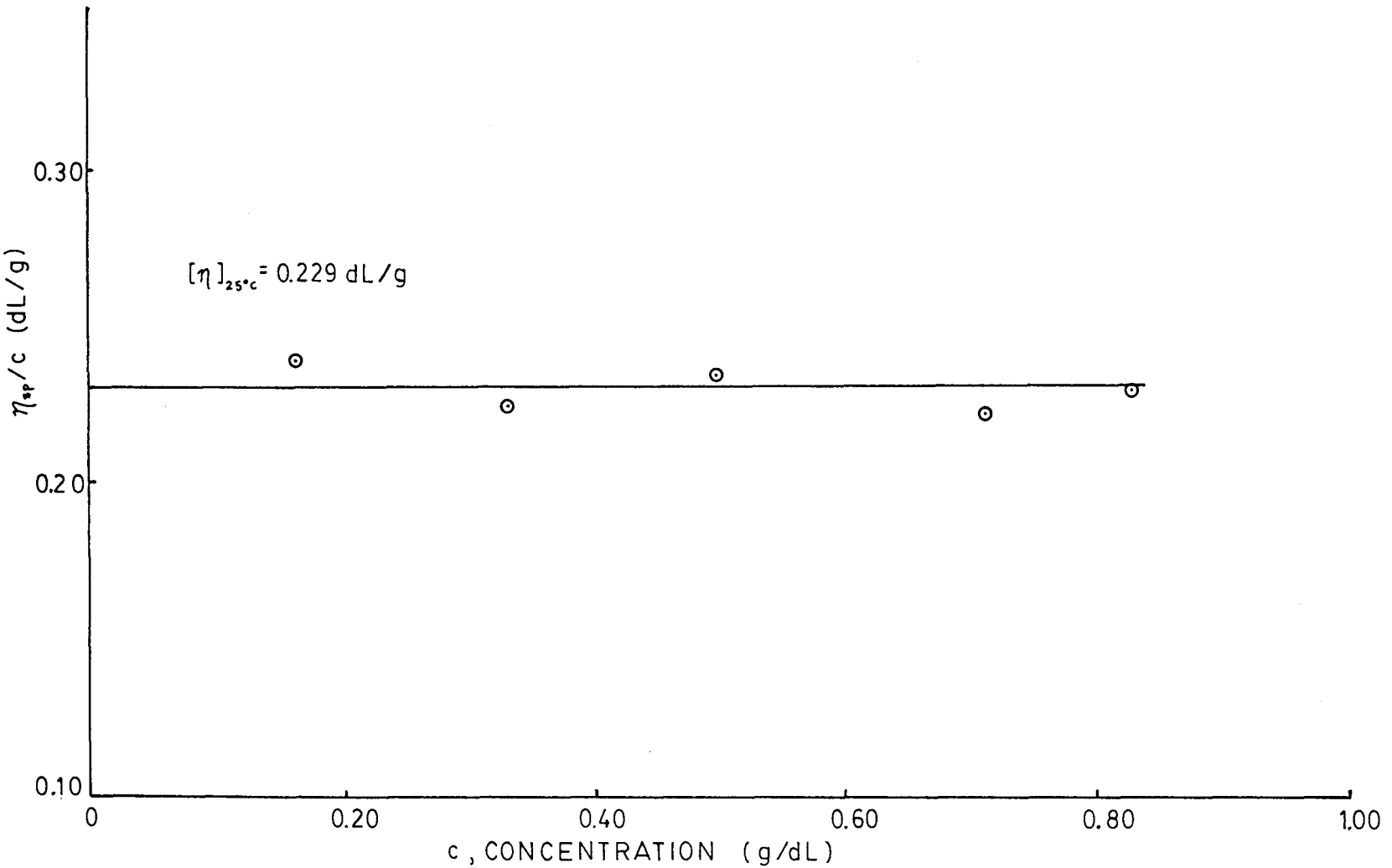

Table I.1 Solution viscosity as a function of PVA-KZ-04 concentration at 25°C.

PVA Concentration (g/dL)	Viscosity (η) (cp)
0	1.0019
0.167	1.0434
0.334	1.0782
0.502	1.1204
0.669	1.1501
0.836	1.1982

APPENDIX II

Film Thickness Measurement Apparatus Assembly and Drop Formation Procedure

The following procedure will describe 1) the method employed to assemble the apparatus used to determine lamella thinning patterns and consequently the film thickness, and 2) the method used to form the drop which is released to the bulk interface.

Once the apparatus was cleaned (section 2.2), the following procedure was used to assemble it (23) (refer to Figure 2.1).

(1) All the reservoirs 11, 12, 13, 14 were filled with their respective liquids.

(2) The cell, 4, was filled with the aqueous solution to a level higher than the drop carrying tube, 6, but lower than the cell cover, 2. The total volume of the cell was approximately 500 mL.

(3) Air was removed from the drop forming device, 8, and conncting tubes, 7. The air was withdrawn with syringe 9, and expelled into the aqueous reservoir, 12. During this procedure the aqueous level in the cell was maintained above the level of the drop carrying tube.

(4) The air from capillary tube 15, was removed by allowing the oil phase to flow through the capillary tube. The air which was now displaced into the connecting tube, 7, was removed by letting the aqueous phase flow from reservoir 12 to the cell, 4.

(5) The cell was filled with butyl chloride, the organic oil, from reservice 13.

(6) The level of the oil/aqueous interface in the cell was adjusted by draining or adding aqueous solution from reservoir 14.

The following procedure describes how butyl chloride oil drops were formed and released to the bulk interface (23) (refer to Figure 2.1).

(1) Alga syringe, 10, was filled with butyl chloride from the oil reservoir, 11.

(2) The two-way stopcock on capillary 15 was opened and the oil forced through the capillary into the drop forming device, 8, with the syringe, 10.

(3) Once the desired drop volume was obtained on the end of the capillary, the stopcock was closed.

(4) The aqueous solution from reservoir 12 was then allowed to flow. This separated the oil drop from the capillary and pushed the drop toward the cell.

(5) A calibrated travelling microscope, was positioned over the connecting tube 7 and was used to determine the drop volume $\pm$ 0.02 µL.

(6) The microscope, 1, was focussed at the bulk interface. Because of the narrow field of view of the microscope, it was necessary to ensure that the drop did not roll. In order to do this, a teflon ring, 3, placed at the interface gave the interface a slight concave shape. Adjustments could be made to the teflon ring by adjusting the screws and cell cover, 2, position.

(7) When interface cleaning was required, the bulk interface was adjusted (section II.1, step 6) such that the tip of the cleaning probe, 5, was just underneath the interface. The stopcock in the probe was then opened and the liquid, equal amounts of oil and aqueous solution, from the interface was removed.

(8) The film thinning between the drop and the interface was photographed on colored slide film, 160 Tungsten ASA, with a Pentax camera mounted on the microscope, 1. The microscope objective was of magnification ten.

APPENDIX III

Surface Tension and Interfacial Tension by the Wilhelmy-Plate Method

A Fisher Autotensiomat^R operating on the principle of the du Nouy ring and Wilhelmy plate methods was employed.

The Wilhelmy plate was suspended from an electromagnetic balance. During a measurement the transducer, which was fixed to the balance beam with a strain-sensitive wire, provided a force-summing displacement signal proportional to the force measured, which in turn was related to the surface or interfacial tension (13).

III.1 Theory

When measuring the surface tension with a partially submerged plate (Figure III.1(a)) which is perfectly wet by the liquid the following force balance applies

$$F = W - B + 2(w+t)\gamma \qquad [III.1]$$

where F is the downward force, W is the weight of the plate, B is the buoyancy force upward, t is the thickness of the plate which is much less than w, the width of the plate, and is therefore ignored. γ is the surface tension.

The Autotensiomat was calibrated according to the instruction manual (13) replacing the du Nouy ring with the Wilhelmy plate.

In this calibration procedure the weight of the plate and hanging wire was first tared, setting $W = 0$, then a 500 mg standard weight was placed on the hanging wire and the recorder set to 98.1 mN/m. This recorder setting is different from that stated in the Fisher instruction manual because of the change from ring to plate.

$$(\gamma = ma/2w = (0.5)(981)/(2(2.50)) = 98.1 \text{ mN/m})$$

Measurements of surface tension were made when the buoyancy force was zero (Figure III.1(b)). Thus equation III.1 becomes

$$F = 2\,w\,\gamma$$

$$\gamma = \frac{F}{2w} \qquad [III.2]$$

When determining interfacial tensions, the instrument was again calibrated as above. Then, the aqueous phase was placed into the sample vessel and the Wilhelmy plate lowered into this phase. Enough butyl chloride to cover the plate, when positioned at the interface, was placed above the aqueous phase, and the two liquids allowed to equilibrate. The plate was then pulled through the aqueous phase into the organic phase. The interfacial tension was measured at the interface (Figure III.1(b)) according to equation III.3.

$$F = -B + 2\,w\,\gamma$$

$$\gamma = \frac{F + B}{2w} \qquad [III.3]$$

III.2 Experimental Procedure

PVA solutions whose concentrations were greater than 0.0300 g/dL were prepared by weight. Those with concentrations less than 0.0300 g/dL were prepared by dilution of the 0.0300 g/dL solution.

Before every run the Wilhelmy plate was cleaned with acetone and then purified water. The glass sample vessel was washed according to the standard procedure (section 2.2).

The liquid in the sample vessel was temperature controlled with circulating water which was thermostated at 25 $\pm$ 0.2°C. Equilibration times were approximately half an hour.

Figure III.1

a) Partially submerged Wilhelmy plate which is perfecty wet by the liquid.

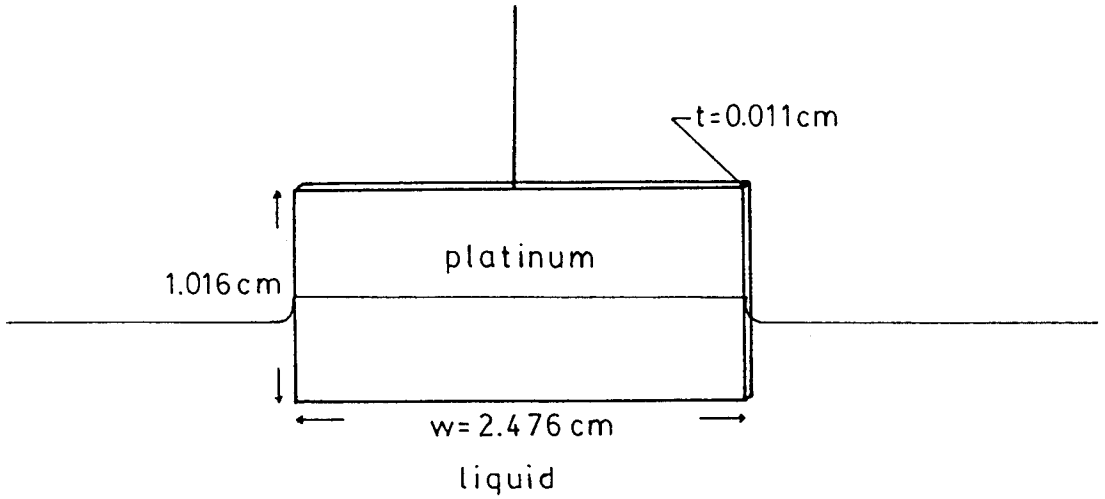

b) Position of Wilhelmy plate when the surface tension of a liquid is measured.

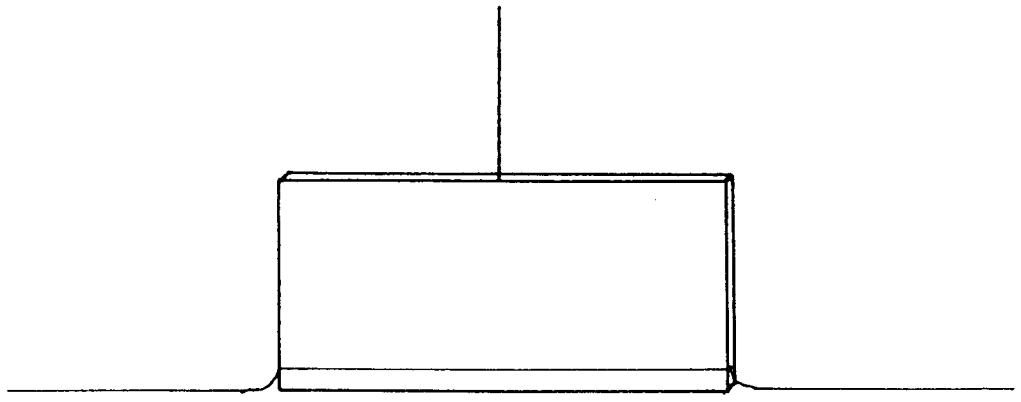

APPENDIX IV

Interfacial Tension by the Drop Weight Method

Figure IV.1 shows the apparatus used to determine the interfacial tension by the drop weight method. This method is based on the fact that the size of drop released from a capillary tip depends on the interfacial tension between the two fluids and their density difference. When the net weight of the liquid in a drop formed on the end of a smooth ground-glass capillary tip exceeds the surface tension force holding the drop to the tip, the drop separates from the tip at the point of minimum cross-sectional area. The equation used to calculate the interfacial tension is (1)

$$\gamma = \frac{mg - \rho Vg}{2\pi r f} \qquad [IV.1]$$

where m is the mass of one drop, g is the force due to gravity, ρ is the density of the liquid, V is the volume of the drop, r is the wetted radius of the capillary tip, and f is a correction factor which is a function of $r/V^{1/3}$.

To obtain the weight of one drop, between ten and twenty drops were released and an average taken. The amount of time required to form and release the drop was approximately two minutes. The aqueous drop contains PVA molecules which are surface active and may not have time to diffuse or rearrange at the interface during the drop formation and release. Thus, the observed interfacial tension may therefore be incorrect. This method is not recommended for the determination of interfacial tensions when surface active agents are present in either phase.

Figure IV.1 Apparatus for the determination of interfacial tensions by the drop weight method.

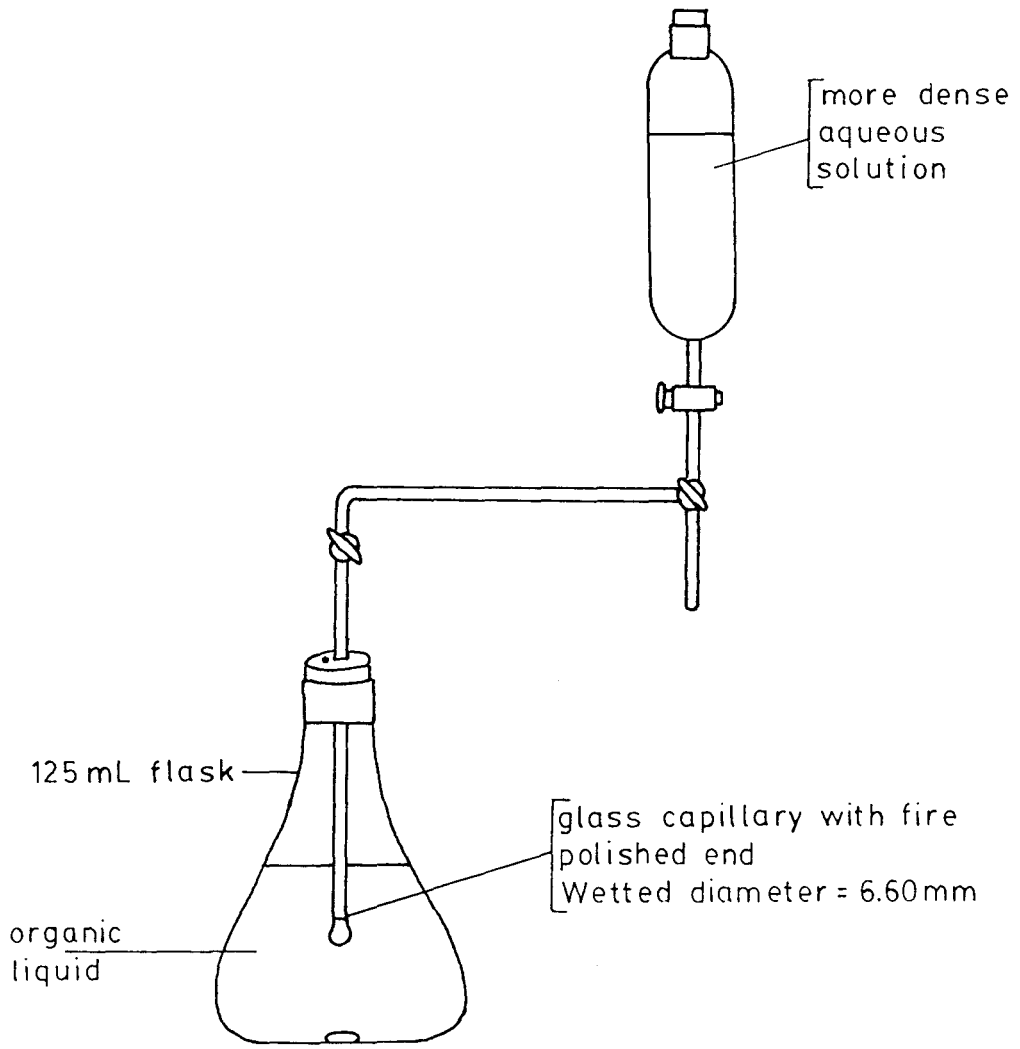

APPENDIX V

Derivation of Equation 3.1

The supply by diffusion of a low-molecular-weight compound to a phase interface can be expressed by the Ward and Tordai equation (47)

$$\eta_t = 2\,c\sqrt{\frac{D}{\pi}}\,\sqrt{t} \qquad [V.1]$$

where

η_t = the number of molecules/unit area which have been supplied to the interface by diffusion at time t.

c = concentration of the low-molecular-weight substance (molecules/volume)

D = diffusion coefficient

t = time during which diffusion has taken place.

Since this equation does not fulfill the condition that the level of adsorption be finite, it is only valid for the initial phase of the adsorption. If we comprise V.1, with the 2-D equation of state $\pi A = kT$ in which π the interfacial pressure is defined as $\gamma_o - \gamma$, then

$$\gamma_t = \gamma_o - 2\,c\,kT\,\sqrt{\frac{D}{\pi}}\,\sqrt{t}\,. \qquad [V.2]$$

where γ_o equals the interfacial tension of the clean interface. Now, since the segment concentration and not the molecular concentration is important for $\Delta\gamma$ in polymer adsorption, then c equals $\nu \cdot c_p$ where ν is the number of segments per molecule adsorbed and c_p is the polymer concentration thus

$$\gamma_t = \gamma_o - 2\,\nu\,c_p\,\sqrt{\frac{D}{\pi}}\,\sqrt{t}\,. \qquad [V.3]$$

$$\gamma_t = \gamma_o - \beta_1\sqrt{t}\,.$$

This equation is similar to equation 3.1.

APPENDIX VI

(1) Gibbs' law as it applies to polymer adsorption (21)

$$\Gamma = \frac{1}{kT}\left(\frac{-d\gamma}{\partial \log c}\right) * \frac{1}{2.30} \qquad [VI.1]$$

where

Γ = adsorbed unit per area

c_p = bulk polymer concentration (assuming subsurface concentration of s.c.e's will be correlated with the bulk polymer concentration)

k = Boltzmann constant

T = absolute temperature

γ = interfacial tension

and by convention the thickness of the interface region is zero and the interface concentration of the solvent is zero.

(2) Combined Theory of Gibbs, Katchalsky and Miller (20)

$$\Delta\gamma = \frac{\delta\, kT}{\bar{P}\, v_s}(0.577 - \frac{\psi}{kT} + \ln V_b) \qquad [VI.2]$$

where

δ = thickness of the boundary layer

V_b = the volume fraction the polymer in the bulk

$\bar{P}$ = degree of polymerization

v_s = volume per segment

ψ = free energy of adsorption per molecule.

δ and ψ are considered to be independent of the bulk polymer concentration.

If we plot γ vs log c_p, according to eq. VI.2, we should obtain a straight line with slope β such that

$$\beta = \frac{\delta k T}{\bar{P} v_s} * 2.30$$

therefore

$$\delta = 0.434 \frac{\beta \bar{P} v_s}{kT} \qquad [V1.3]$$

(3) Combined theory of Gibbs, Frisch and Simha (15)

$$\frac{d\pi}{d(\ln c_p)} = \frac{-kTz}{2A_0 \nu (1 - \frac{1}{\bar{P}})}$$

or

$$\nu = \frac{-kTz}{2A_0 \frac{d\pi}{d(\ln c_p)}} \qquad [V1.4]$$

where

ν = number of segments per polymer adsorbed in the interface

z = coordinates number of the polymer segment in the interface

A_o = limiting surface area per segment

π = interfacial pressure

thus

$$\nu = \frac{z}{2A_0\Gamma} \qquad [V1.5]$$

Figure VI.1 Interfacial tension as a function of PVA concentration.
(Reproduced from Figure 3.1c)

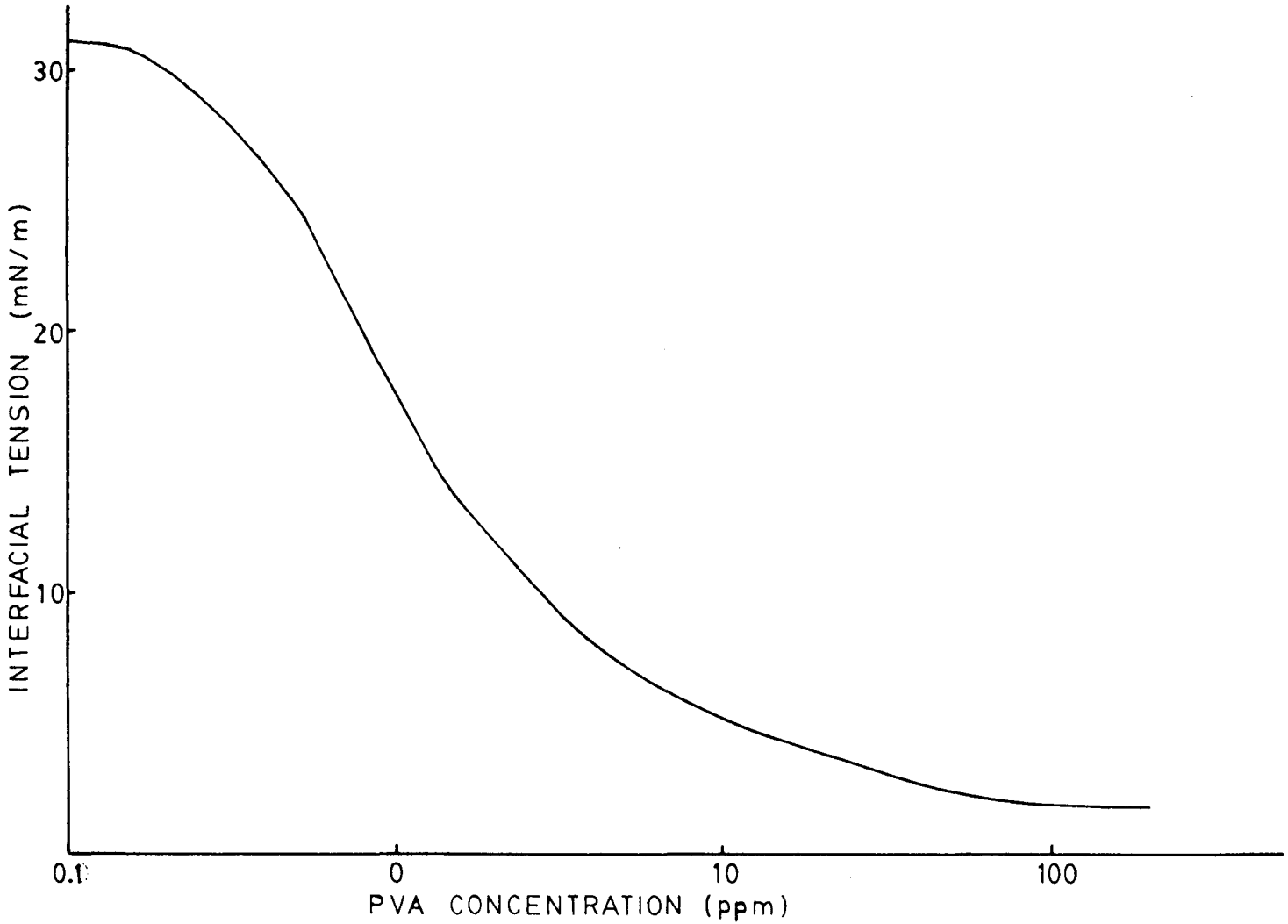

APPENDIX VII

Average Film Thickness Data as a Function of Time from Drop Release

Tables VII.1 and VII.2 list the average film thickness of the lamella as a function of time (T_R) from drop release to the bulk interface for variousPVA-KZ-04 concentrations and drop volumes. This experimental data was obtained using the procedures listed in Appendix II.

Table VII.1 Average film thickness data as a function of time elapsed from drop release. (Baker TM Grade n-butyl chloride)

PVA Concentration (ppm)	Drop Volume (μL)	Average Thickness (nm)	Time (s)
3.11	1.58 to 1.98	130*	120
62.0	1.00	700	90
		300	260
		190	490
		120	645
		90	890
		80	1550
	1.17	500	105
		175	510
		140	780
		125	1165
		125	1590
		125	2280
	1.74	900	60
		500	175
		120	855
		110	1000
		80	1275
		*	1800
	2.78	1000	80
		300	145
		195	250
		120	445
	1.33 & 1.42	750	90
		180	330
		140	530
		120	775
		120	1163
310.	2.46	600	60
		500	85
		220	150
		40	275
		*	345
	0.64	800	40
		120	150
		80	275
		*	720

Table VII.1 Continued

PVA Concentration (ppm)	Drop Volume (μL)	Average Thickness (nm)	Time (s)
310.	1.90	500	60
		270	120
		210	157
		150	255
		70	320
		40	420
		*	760
	3.02	300	157
		180	243
		140	323
		120	397
		*	590
620.	1.41	210	120
		85	290
		60	420
		40	540
		*	645
	3.42	600	120
		140	300
		100	360
		60	420
		*	630
	1.49	700	70
		450	130
		350	257
		110	365
		60	440
		*	640
	1.01	220	95
		140	160
		60	290
		*	500

* coalesced

Table VII.2 Average film thickness data as a function of time elapsed from drop release. (Baker Analyzed n-butyl chloride)

PVA Concentration (ppm)	Drop Volume (μL)	Average Thickness (nm)	Time (s)
300.	2.13	280	155
		210	325
		185	425
		170	683
	1.40	235	130
		210	215
		190	325
		160	800
	2.45	500 or 300	130
		240	310
		170	655
600.	1.00	280	95
		100	157
		90	217
		80	315
	3.58	1000	70
		400	195
		120	300
		50	360
		*	390
1200.	2.05	400	85
		250	105
		130	244
		70	310
		*	360
	3.42	1100	55
		700	157
		130	265
		70	380
		*	450

* coalesced

REFERENCES

1. Adamson, A.W., 'The Physical Chemistry of Surfaces', John Wiley and Sons, Toronto, p. 22 (1982).

2. Böhm, J.Th., 'Adsorption of Polyelectrolytes at Liquid-Liquid Interfaces and Its Effect on Emulsification', Ph.D. Thesis, Agricultural University, Wageningen, The Netherlands (1974).

3. Burrill, K.A., 'Coalescence in Oil/Water Systems', Ph.D. Thesis, McMaster University, Hamilton, Canada (1970).

4. Cohen Stuart, M.A., 'Flexible Polymers at a Solid-Liquid Interface', Ph.D. Thesis, Agricultural University, Wageningen, The Netherlands (1980).

5. CRC Handbook of Chemistry and Phuysics, Weast, R.C., Ed. (1974).

6. De Vries, A.J., Recueil de Travaux, 77, 81-91, 209-223, 283-296, 383-399, 441-461 (1958).

7. Di Marzio, E.A. and Rubin, R.J., J. Chem. Phys., 55, 4318 (1971).

8. Dolan, A.K. and Edwards, S.F., Proc. R. Soc. Lond., A. 337, 509-516 (1974).

9. Dolan, A.K. and Edwards, S.F., Proc. R. Soc. Lond., A. 343, 427-443 (1975).

10. Evans, R. and Napper, D.H., MTP Review of Science, vol. 7, M. Kerker, Ed., Series I, 241 (1972), Series II, 194 (1975).

11. Flory, P.J., 'Principles of Polymer Chemistry', Cornell University Press, Ithaca, 611 (1953).

12. Fischer, E.W., Kolloid Z., 160, 120 (1958).

13. Fisher Scientific Co. Manual, 'Fisher Model 215 Autotensiomat Surface Tension Analyzer' (1976).

14. Frankel, S.P. and Mysels, K.J., 'Soap Films - A Study of Their Thinning', Pergamon Press, London (1959).

15. Frisch, H.L. and Simha, R., J. Chem. Phys., 27, 702-706 (1957).

16. Hesselink, F.Th., Journal of Polymer Science, Polymer Symposium, John Wiley and Sons Inc., 61, 439-449 (1977).

17. Hesselink, F.Th., Vrij, A. and Overbeek, J.Th.G., J. Phys. Chem., 75, 2094 (1971).

18. Hodgson, T.D. and Woods, D.R., J. Colloid and Int. Sci., 30 (4), 429-446 (1969).

19. Huggins, M.L., ACS, 64, 2716 (1942).

20. Katchalsky, A. and Miller, I., J. Phys. Chem., 55, 1182-94 (1951).

21. Lankveld, J.M.G., 'Adsorption of Polyvinyl alcohol on Paraffin - Water Interfaces and the Properties of Paraffin-in-Water Emulsions Stabilized by Polyvinyl Alcohol', Ph.D. Thesis, Agricultural University, Wageningen, The Netherlands, 70 21 (1970).

22. Lawrence, A.C.S., 'Soap Films', Bell and Sons, London (1929).

23. Liem, A.J.S., 'Film Thinning in Oil/Water Coalescence', Ph.D. Thesis, McMaster University, Hamilton, Canada (1975).

24. Li-In-On, F.K.R., Vincent, B. and Waite, F.A., In 'Colloidal Dispersions and Micellar Behavior', K.L. Mittal, Ed., ACS Symposium, Series 9, Washington, DC, 165-172 (1975).

25. MacKay, G.D.M. and Mason, S.G., Can. J. Chem. Eng., 41, 203-212 (1963).

26. Mackor, E.L., J. Colloid Sci., 6, 942 (1951).

27. Meier, D.J., J. Phys. Chem., 71, 1861 (1967).

28. Napper, D.H., In 'Colloidal Dispersions' J.W. Goodwin, Ed., The Royal Society of Chemistry, London, p. 99 (1982).

29. Napper, D.H., J. Colloid Interface Sci., 32, 106 (1970).

30. Napper, D.H., Trans. Faraday Soc., 64, 1701 (1968).

31. Princen, H.M. and Mason, S.G., J. Coll. Sci., 20, 156 (1965).

32. Princen, H.M., Zia, I.Y.Z. and Mason, S.G., J. Colloid and Int. Sci., 23, 99 (1967).

33. Private Communications, Andrews, P., Chemistry, McMaster University, Hamilton (1983).

34. Private Communication, Imperial Oil Ltd., Sarnia.

35. Sato, T. and Ruch, R., 'Stabilization of Colloidal Dispersions by Polymer Adsorption', Marcel Dekker, Inc., New York (1980).

36. Scheutjens, J.M.H.M. and Fleer, G.J., Advances in Colloid and Interface Science, 16, 361-380 (1982).

37. Scheutjens, J.M.H.M. and Fleer, G.J., J. Phys. Chem., 84, 178-190 (1980).

38. Scheutjens, J.M.H.M. and Fleer, G.J., J. Phys. Chem., 83, 1619-1635 (1979).

39. Schick, M.J. and Harvey, E.N. Jr., In Adv. Chem. Ser. 87, chap. 5 (R.F. Gould, ed.), Am. Chem. Soc. (1968).

40. Scholtens, B.J.R., 'Copolymers at a Liquid-Liquid Interface and Their Retarding Effect on Mass Transfer Between Both Phases', Ph.D. Thesis, Agricultural University, Wageningen, The Netherlands, p. 16-17 (1977).

41. Toyoshima, K., Soc. Chem. Ind. Monograph nr. 30, 154-187 (1968).

42. Tregan, R. and Bonnemayre, A., Rev. Plast. Mod., 23, 7 (1970).

43. Van der Linden, C. and Van Leemput, R., J. Colloid Interface Sci., 67, 48 and 63 (1978).

44. van Vliet, T., 'Interactions Between Adsorbed Macromolecules', Ph.D. Thesis, Agricultural University, Wageningen, The Netherlands, 77-1, p. 14 (1977).

45. Vonnegut, B., Rev. Sci. Intstr., 13, 6 (1942).

46. Vrij, A. and Overbeek, J.TH.G., J.A.C.S., 90, 3074-3078 (1968).

47. Ward, A.F.H. and Tordai, J. Chem. Phys., 14, 453-461 (1946).

48. Fleer, G.J., Koopal, L.K. and Lykleman, J., Kolloid Z.Z. Polym. 250, 689-702 (1972).